

**Simulation of Syngas Production via Carbon Dioxide Reforming of Methane in a
Fluidized Bed Reactor**

By

Mohd. Farhan Hatta bin Husain

Dissertaion submitted in partial fulfillment of
The requirement for the Bachelor (Hons)
(Chemical Engineering)

NOVEMBER 2002

Universiti Teknologi PETRONAS
Bandar Seri Iskandar
31750 Tronoh
Perak Darul Ridzuan

t
TP
761
M4
M697
2002

1. Methane
2. Carbon dioxide
3. CE -- Thesis

CERTIFICATE OF APPROVAL

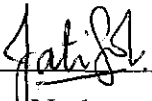
Simulation of Syngas Production via Carbon Dioxide Reforming of Methane in a Fluidized Bed Reactor

By

Mohd. Farhan Hatta bin husain

A project dissertation submitted to the
Chemical Engineering Programme
Universiti Teknologi PETRONAS
In partial fulfillment of the requirements for the
BACHELOR OF ENGINEERING (Hons)
(CHEMICAL ENGINEERING)

Approved by



(Miss Nurhayati Mellon)

UNIVERSITI TEKNOLOGI PETRONAS
TRONOH
November 2002

TABLE OF CONTENTS

ABSTRACT	i
ACKNOWLEDGEMENT	ii
ABBREVIATION AND NOMENCLATURE	iv
CHAPTER 1: INTRODUCTION	1
1.1 Background	1
1.2 Problem Statement	2
1.3 Objectives and Scope of Study	3
CHAPTER 2: LITERATURE REVIEW AND THEORY	4
2.1 The reaction	4
2.2 Reaction Kinetics	4
2.3 Reactor design.	9
CHAPTER 3: PROJECT WORK AND METHODOLOGY.	10
CHAPTER 4: DISCUSSION.	11
4.1 Rate of Reaction	11
4.2 Design Equation	12
4.3 Modeling	13
4.4 Concentration Profile	14
4.5 Validity of Assumptions	17
4.6 Other Tests	18
CHAPTER 5: CONCLUSION	20
CHAPTER 6: REFERENCES	21

CHAPTER 7:	APPENDICES	23
	7.1 Gant-Chart	24
	7.2 Case Study Journal	25
	7.3 Matlab Programming	38

Abstract

The paper produced is to present the simulation results of an experiment. The experiment is about the reaction engineering of carbon dioxide reforming of methane in a fluidized bed reactor. The model to be constructed will be used to analysed mechanism and activity of the reaction.

Carbon dioxide reforming is the latest method of obtaining syngas a valuable feedstock for many petrochemical industries. The product varies from naphtha to diesel and fuel additives in automotive industry.

The project involves a study on surface engineering that is catalytic mechanism and activity of the process. Generally the study is based on a journal, which has been selected as the case study. Upon understanding of the basic mechanism, a simple simulation will be carried out for the selected process.

Extensive literature review will give sufficient information towards the development of the model. Some calculations were made in order to obtain some parameters and variables, which will be used in the computer simulation.

From the model created, it is found that the concentration profile along the catalyst bed drops at a very high rate before slowing down. Factors affecting the behavior of the reactant concentration will be discussed further.

Acknowledgement

In the Name of Allah Most Gracious Most Merciful

Praise be to Allah Lord of the Worlds

Most Gracious Most Merciful

Owner of the Day of Judgement

Thine aid we seek

Show us the straight path

The path of whom thou hast favored

Not of those who earn Thine anger nor of those who go astray

Many at hand have encourage me from all aspect of project development. My acievement lie not only within my desire to perform but also a burning fire rekindled by parties of whom we feel greatly gratified to. Rendering me with guidance, support and love which are vital elements of this project and for spiritual harmony. These parties are as follows:

Miss Nurhayati Mellon, lighting a fire that surely inspires and light the path of which is taken, Winding roas then seem straightened and restless wandering minds soon enlightened. Utmost gratitude I shower upon her for brightening up what was once dim...

Thank you for all the guidance and insights shown throughout the entire course duration. I shall kept all the knowledge obtained in my mind as ideas and in my heart as inspiration.

My parents, morning comes showering light, unto the earth blissful bright, and which lays a never ending care showered by dew and warm sea brew. A care shown for seedlings sown are those shown by parents grown, never ending never less, always loving entirely blessed...

My humble gratitude and love to my parents for their support in completing this project.
My success is their pride and my achievement is their smile.

And to other parties that may have contributed to us in any form we humbly offer a word
of gratitude. Thank you.

Abbreviation and Nomenclature

C_b	Concentration at carbon dioxide at bubble phase, ppm
C_e	Concentration of carbon dioxide at emulsion phase, ppm
d_p	particle diameter, μm
D_{eff}	effective diffusivity, cm^2/s
D_{ze}	dispersion coefficient in emulsion phase, m^2/s
f_b	bed fraction covered by bubbles phase
f_e	bed fraction covered by emulsion phase
g	earth acceleration, m s^{-2}
g_b	mass of solid in bubble phase, kg/m^3
g_e	mass of solid in emulsion phase, kg/m^3
h	bed height, m
k_{CO_2}	interchange coefficient, atm^{-2}
k	adsorption constant, atm^{-1}
k_1	mass transfer coefficient, m
m	mass of catalyst, g
p_{CH_4}	partial pressure of methane, kPa
p_{CO_2}	partial pressure of carbon dioxide, kPa
p_{CO}	partial pressure of carbon monoxide, kPa
ρ_s	catalyst solid density, g cm^{-3}
ρ_g	gas density, g cm^{-3}
r_{CO_2}	rate of reaction of carbon dioxide, $\text{mol s}^{-1} \text{kg}_{\text{cat}}^{-1}$
u_b	bubble velocity, m/s
u_{mf}	minimum fluidization velocity, m/s

1 INTRODUCTION

1.1 Background

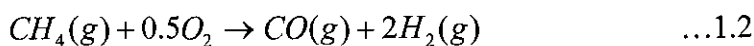
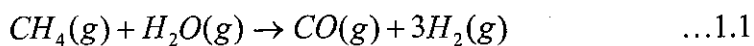
Methane is a single tetravalent carbon atom surrounded by four hydrogen atoms arranged in a tetrahedral geometry. Methane is extremely important as it can be considered as the "parent" of organic chemistry. All organic compounds are methane with the hydrogen atoms replaced by other atoms or functional groups.

Methane is a flammable, odorless, non-toxic gas formed naturally by bacteria, which release single carbon atoms from digested organic material. It occurs as marsh gas when it is not trapped by rock and it is the main component of natural gas. When methane is burnt in air, the hydrogen atoms are stripped from the carbon by oxygen to form water molecules, while the carbon quickly reacts to form carbon dioxide molecules.

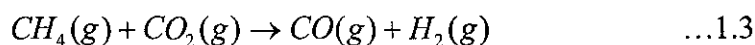
Gas to Liquid (GTL) technology is a paradigm shift of petrochemical processes. It partially solves the problem of extinction of hydrocarbon resources by generating liquid hydrocarbon from gas hydrocarbon.

GTL comprises of two distinct and separate processes. Hydrocarbon gas that is methane will first react to form synthesis gas also known as syngas. This syngas is a mixture of hydrogen and carbon monoxide. This is the main feedstock for Fischer-Tropsch process where syngas is converted to a long chain liquid hydrocarbon. The GTL products are referred as synfuels ranging from naphtha to diesel.

Two common method of producing syngas is steam reforming and partial oxidation of methane. Steam reforming is denoted by equation (1.1) while partial oxidation is denoted by equation (1.2).



Latest discovery of syngas production is carbon dioxide reforming of methane as given below:



1.2 Problem statement

Currently syngas is mainly produced mainly by steam reforming and partial oxidation of methane. Recent discovery of carbon dioxide reforming of methane has attracted renewed global interest. An advantage of producing synthesis gas by carbon dioxide reforming instead of processes such as steam reforming and partial oxidation is the low H₂: CO ratio obtained, which is of particular interest to the synthesis of valuable oxygenated chemicals.

The carbon dioxide reforming offer some other important advantage compared to other synthesis gas production. The low ratio of H₂: CO is favorable for Fischer-Tropsch synthesis. It also reduces carbon dioxide and methane emission, which are both greenhouse gases. Yet, the reaction still has no commercial application. This is due to the economics of the reaction, which have very high requirements.

Major disadvantage of carbon dioxide reforming is the high thermodynamic potential in coke formation. A lot of effort has been directed towards the development of the reaction. This involves study on the usage of catalysts, reactors and other reaction conditions in order to acquire optimum reaction condition, where highest yield can be achieved at lowest condition requirement.

1.3 Objective and Scope of Study

The main objective of this project is to model the reaction of carbon dioxide reforming of methane. The reaction model shall be tested and the result will be analyzed on the behavior of the reactants. In order to model the equation, a study on the reaction mechanism is required. After obtaining the reaction rate equation, the design equation will be derived based on type of reactor used. The reaction model will be constructed by using Matlab.

All experimental data for the case study in this project is based on a selected journal from a variety of journals obtained through the library and the Internet. Decision is made based on the information included in the journal.

Development of carbon dioxide reforming reaction model require an extensive studies. Focus is given on the reaction mechanism, which will involve adsorption and desorption on the catalyst surface. The type of catalyst used and the ways the catalyst behaves towards the reaction will also be studied. The study will also covers on the kinetics of the reaction where the rate of reaction will be determined.

Understanding the reaction mechanism will give the factors that influence the yield of that reaction. This includes type of reactors used and the reaction condition that will influence the reaction. Information obtained from this study will be used later to develop the design equation to model the synthesis gas production.

Familiarization of computer software, Matlab is crucial in order to make the project successful. Modelling of the reaction will be performed using Matlab. From this model, optimum condition of the reaction could be estimated based on validity of assumptions made in deriving the model.

2 LITEATURE REVIEW AND THEORY

2.1 The reaction

Carbon dioxide reforming of methane will produce carbon monoxide and hydrogen using one percent of nickel on alumina oxide catalyst. This process is more preferred compared to steam reforming and partial oxidation due to the low H₂: CO ratio of 1:1 which is desirable for Fischer-Tropsch synthesis.



As been stated above, the reaction is endothermic, which require a good temperature control reactor system to ensure sufficient heat is provided for the reaction. The reaction is performed at 800°C inside a laboratory-scale fluidized bed reactor. Information on the fluidized bed reactor will be explained in the later part of the chapter.

2.2 Reaction Kinetics

The rate of reaction can be expressed as a change of concentration of methane and carbon dioxide with time. The reaction rate is given as

$$r = \frac{-d[CH_4]}{dt} = \frac{-d[CO_2]}{dt} = k[CH_4][CO_2]^2 \quad \dots 2.2$$

The reaction is a second order reaction with respect to both carbon dioxide and methane. The determination of the rate law is based on concentration of reactants. Further integration of equation 2 gives

$$\ln \frac{[CO_2]_0}{[CO_2]} = kt([CH_4]_0 - [CO_2]_0) + \ln \frac{[CH_4]_0}{[CH_4]} \quad \dots 2.3$$

The equation can be plotted on a graph as $y = mx + c$. The alternative way of describing this second order process of this type is by using extent of reaction, x . If the same reaction occur, having both reactant at the same amount,

$$\frac{dx}{dt} = k(a - x)(b - x) \quad \dots 2.4$$

Integration gives

$$\frac{1}{b - a} \ln \frac{a(b - x)}{b(a - x)} = kt \quad \dots 2.5$$

However these methods applies if there is no catalyst present in the reaction. [3] Catalyzed reaction will involved adsorption and desorption of reactants (carbon dioxide and methane) and products (syngas) which on solid catalyst surface (nickel). This is called heterogeneous catalysis where a solid (catalyst) has gaseous reactant attached to it and subsequently react. Heterogenous catalysed reaction involves the possibility of either or both reactant and product of reaction being adsorb or desorb on the catalyst surface. The nickel catalyst impregnated in alumina oxide carrier functioned to enhance rate of reaction by lowering activation energy for the reaction and increase selectivity of desired product.

Heterogeneous catalytic reaction involves several different steps. The reaction occur when reactant (carbon dioxide and methane) flow through bed of catalyst and absorbed to the catalyst active site (nickel) before being converted to product. [2] In order for conversion of carbon dioxide and methane to syngas these viable steps must occur:

- Transport of carbon dioxide and methane from the bulk fluid to the stagnant film surrounding catalyst particle
- Diffusion of both carbon dioxide and methane into alumina oxide catalyst pores
- Adsorption of reactants (carbon dioxide and methane) onto nickel active site surfaces

- Reaction of carbon dioxide and methane to syngas on the nickel surfaces
- Desorption of products (syngas) through porous alumina oxide to its pore mouth
- Transport of syngas from the stagnant film around the catalyst to bulk fluid

In the carbon dioxide reforming of methane, both carbon dioxide and methane will adsorb on the surface of catalyst active site while syngas desorb from it continuously. There are 2 types of adsorption; physical and chemical adsorption. [4]

Physical adsorption is weak forces between adsorbate and adsorbent. It usually occurs because of condensation of reactants on catalyst surface. Meanwhile, chemisorption releases high energy during adsorption and this energy will give the reactants energy to overcome the reaction activation energy barrier. That is why reaction is always linked to chemisorption and not physical adsorption.

Since the reaction involves catalytic activity, the rate of reaction is developed based on adsorption isotherm. Langmuir proposed simple formulation for adsorption and desorption of gases on solid catalyst surface. The formula was derived based on several important assumptions:

- All the surface of the active site of the catalyst is uniform. This will make the adsorption and desorption have the same activity or rate.
- The amount of reactant adsorbed has no effect on further rate of adsorption.
- Adsorptions occur with the same mechanism and adsorbed reactants possess similar structure
- The adsorption which is mainly chemisorption is limited to monomolecular layer on the active site surface.

The adsorption and desorption process will continuously occur and eventually an equilibrium between both processes will be established. Therefore, the rate of adsorption, r_a will equal to rate of desorption r_d . [2] Rate of adsorption is equal to

$$r_a = kp(1 - \theta) \quad \dots 2.6$$

Where k is a constant involving proportionality between r_a and p , pressure of the reactants. Since the adsorption is limited to monomolecular layer, the surface is presented by fraction θ covered by adsorbed reactants and $1-\theta$ which is bare. Meanwhile the rate of desorption is presented by:

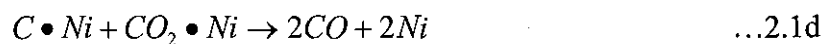
$$r_d = k'\theta \quad \dots 2.7$$

Due to equilibrium, equation 2.6 is equal to reaction 2.7. The resulting equation is given by:

$$\theta = \frac{kp}{k'+kp} = \frac{K_p}{1 + K_p} \quad \text{where } K_p = k/k' \quad \dots 2.8$$

The determination of rate of reaction is now getting more complicated. This is because the seven step of reaction involving adsorption, diffusion and desorption must be taken into consideration.

Every reaction actually comprises of several elementary step. These elementary steps will present the adsorption, reaction and desorption process during the reaction. These are elementary steps of carbon dioxide reforming of methane, equation 1



Since the reaction occur in series, the slowest or rate determining step will determine the overall reaction rate. Rate determining step is the slowest elementary steps and controls overall rate of reaction. In this reaction, the rate determining step is equation 1d, where reaction is the rate determining step or the rate controlling reaction. [12]

Since the surface reaction controlling case is generally the most important for industrial conditions, the discussion of bimolecular reactions will be restricted to this case. There are two different mechanism for bimolecular surface-catalyze reactions. [2]

1. The Langmuir-Hinshelwood mechanism for the reaction of two adsorbed surface species to products.
2. The Rideal-Eley mechanism for the reaction of a gas phase species with an adsorbed species to products.

Reaction rate of carbon dioxide reforming was calculated using a Langmuir-Hinshelwood rate expression. The rate expression for carbon dioxide reforming is

$$r_{CO_2} = k_1 C_{CH_4-Ni} C_{CO_2-Ni} - k_2 C_{CO-Ni} C_{H_2-Ni}$$

$$= \frac{k'_1 k_{CH_4} k_{CO_2} P_{CH_4} P_{CO_2} - k_{CO} k_{H_2} P_{CO} P_{H_2}}{(1 + k_{CH_4} P_{CH_4} + k_{CO_2} P_{CO_2})(1 + k_{CO} P_{CO} + k_{H_2} P_{H_2})} \quad \dots 2.9$$

where

$$k'_1 = k_1 n_1 n_2 \quad \text{and} \quad k'_2 = k_2 n_1 n_2$$

Further derivation will give

$$r_{CO_2} = \frac{k_{CO_2} - P_{CH_4} P_{CO_2}}{(1 + k_1 P_{CH_4} + K_2 P_{CO})(1 + k_3 P_{CO_2})} \quad \dots 2.10$$

where all the k and P variables represent for the coefficient of each substance that take part in the reaction.

2.3 Reactor Design

Fluidized bed reactors involve catalyst beds, which are not packed rigid but suspended in fluid. Flow through bed is upward to reduce pressure drop at high velocity. At high velocity, the frictional drag force on particles becomes greater than their weight thus the bed start to expand. As the velocity increases, the bed seems to loose its form and is fluidized. [6]

The advantage of having fluidized bed reactor is that the reactor offers good mixing of particles. Intimate mixing and rapid heat transfer ensures easy control of reactor temperature. Fluidized bed also works with finer catalyst particles since pressure drop is no longer a problem.

The model is based on the two-phase theory of fluidization. According to the theory, the bed is divided into two phases; emulsion and bubble phases. Gas flows through the emulsion phase with the minimum fluidization velocity. The excess gas flows in the form of bubbles. The bubbles phase consists of particle-free bubbles. The hydrodynamics for both phases can be modeled as below

Equation for bubble phase,

$$u_b A f_b C_{Ab} \Big|_z - u_b A f_b C_{Ab} \Big|_{z+\Delta z} + k_1 (C_{Ab} - C_{Ae}) A \delta z + g_b f_b r_A' A \delta z = 0 \quad \dots 2.11$$

$$u_b A f_b \frac{dC_{Ab}}{dz} + k_1 C (C_{Ab} - C_{Ae}) + g_b f_b r_A' = 0$$

Equation for emulsion phase,

$$u_e A f_e C_{Ae} \Big|_z - u_e f_e A C_{Ae} \Big|_{z+\Delta z} + A f_e D_{ze} \frac{dC_{Ae}}{dz} \Big|_z - A f_e D_{ze} \frac{dC_{Ae}}{dz} \Big|_{z+\Delta z} - k_1 (C_{Ab} - C_{Ae}) A \Delta z + g_e (1 - f_b) r_A' = 0$$

$$u_e f_e \frac{dC_{Ae}}{dz} - f_e D_{ze} \frac{d^2 C_{Ae}}{dz^2} - k_1 (C_{Ab} - C_{Ae}) + g_e (1 - f_b) r_A' = 0 \quad \dots 2.12$$

3. PROJECT WORK AND METHODOLOGY

Initial stage of the project require an understanding of the fundamental and knowledge about the reaction. This is done through references from books, journal, article and website. This method is a preliminary to the literature research. Literature reviews will give depth to the project where most of the discussion will be backup by these information.

The project basically is a further study of a journal entitled “Reaction Engineering Investigations of CO₂ Reforming in a Fluidized Bed Reactor”. Please refer appendix 1 for the journal. The paper will be taken as case study and the experimental data from it will be used in the later stages of this project which is modeling. The whole research initiates from the paper and other related topics will be included as further knowledges.

The study will involve some calculation where rate of reaction and the design equation for the whole process will be determined. The results from calculation will be discussed and used as assumptions to solve for problems encountered in the later stage of the project.

The final part of the project is simulation of the carbon dioxide reforming. A model of the reaction will be constructed using computer software, which is Matlab. The model will give opportunity for users to find the best combination of reaction condition in order to achieve highest yield.

Summary of project activity can be referred in the project Gant-Chart. Please refer Appendix 2 for the project Gant-Chart.

4 DISCUSSION

4.1 Rate of reaction

Currently the reaction rate includes the surface reaction and the mass transfer terms. The reaction rate depends on the controlling reaction step. In order to determine the controlling reaction step, Thiele modulus ϕ , should be known. This is done using equation

$$\phi_{pore} = L \left(\frac{k\rho_s}{D_{eff}} \right)^{1/2} = 0.1628 < 0.4 \quad \dots 4.1$$

Catalyst pores length, $L = 40 \text{ E}^{-12} \text{ m [J]}$

Diffusion coefficient, $K_{\text{CO}_2} = 0.0150$

Effective Diffusivity, $D_{eff} = 0.163 \text{ cm}^2/\text{s [P]}$

For Thiele modulus smaller than 0.4, the drop in concentration of reactants through the pore is small, whereas for Thiele modulus larger than 0.4, the reactants concentration drop is large. [2]

From the calculation above, it is found that the Thiele modulus is smaller than 0.4 indicating that the reaction is the slower step or the rate determining step. Thus the mass transfer diffusion can be neglected.

There is another reason for the neglecting mass transfer diffusion terms in order to model the catalytic mechanism for the reaction. Since the particle size of the catalyst is small, ($\rho_s=110\mu\text{m}$) there will be no diffusion of reactant through the pores of catalyst particle. Hence the mass transfer diffusion terms can be totally left behind. [5]

4.2 Design Equation

At high velocity, the fluidization may become more vigorous. The situation may lead to big bubbles thus creating slugs of gas, which occupies the entire cross section of the bed. Thin bubble formation could cause extinction of the emulsion phase. To prove this, the minimum fluidization velocity must be calculated and then compared with the bubble phase velocity.

The volume of reactor, V and the catalyst particle density ρ_s , must first be determined to perform minimum fluidized velocity calculation.

$$V = \pi \left(\frac{d^2}{4} \right) h = 3.142 \left(\frac{5}{2} \right)^2 5 = 98.175 \text{ cm}^3 \quad \dots 4.2$$

Diameter of reactor, $d = 5 \text{ cm}$ [9]

Height of catalyst bed, $h = 5 \text{ cm}$ [9]

Catalyst particle density, ρ_s

$$\rho_s = \frac{m}{V} = \frac{177.2 \text{ g}}{98.175 \text{ cm}^3} 1.805 \text{ g cm}^{-3} = 1805 \text{ kg m}^{-3} \quad \dots 4.3$$

Total mass of catalyst, $m = 140 \text{ g}$ [9]

Minimum fluidized velocity, U_{mf}

$$u_{mf} = \frac{1}{180} \frac{\varepsilon_{mf}^3 - d_p^2 (\rho_s - \rho_g) g}{1 - \varepsilon_{mf} \mu} = 0.006 \text{ ms}^{-1} \quad \dots 4.4$$

Bed porosity, $\varepsilon_{mf} = 0.4$, assuming for a bed of isometric particles [6]

Average catalyst particle diameter, $\rho_s = 110 \mu\text{m}$ [9]

Gas density $\rho_g = 0.3135 \text{ g cm}^{-3}$ [1]

Viscosity $\mu = 1.445 \times 10^{-7} \text{ cp}$ [1]

Bubble velocity, u_b

$$\text{fluidizationnumber} = \frac{u_b}{u_{mf}} \quad \dots 4.5$$

$$u_b = \text{fluidizationnumber} * u_{mf} = 11.8 * 0.006 \text{ m/s} = 7.1 \text{ m/s}$$

Huge bubble velocity compared to minimum fluidized bed, $u_b \gg u_{mf}$, ($u_b = 7.1 \text{ m/s}$; $u_{mf} = 0.06 \text{ m/s}$) shows the rigorous mixing in the emulsion phase. [6] The huge differences between both bubbles and minimum velocity proves that there is no emulsion phase presents. Thus emulsion phase equation of the fluidized bed (equation 2.12) will be reduced to

$$K_1(C_{Ab} - C_{Ae}) = (1 - f_b)g_e r_a \quad \dots 4.6$$

4.3 Modeling

The reaction is modeled by the design equation of the reaction. The rate of reaction (equation 2.10) will be fitted into the design equation (equation 2.11 and 4.6). All the experimental values are substituted into the formula. Concentration profile of carbon dioxide along the catalyst bed will be investigated using the simulation model. The initial concentration of carbon dioxide is 100 ppm and the concentration will be tested through a catalyst bed of 5 cm height. The Matlab coding can be found in appendix 3.

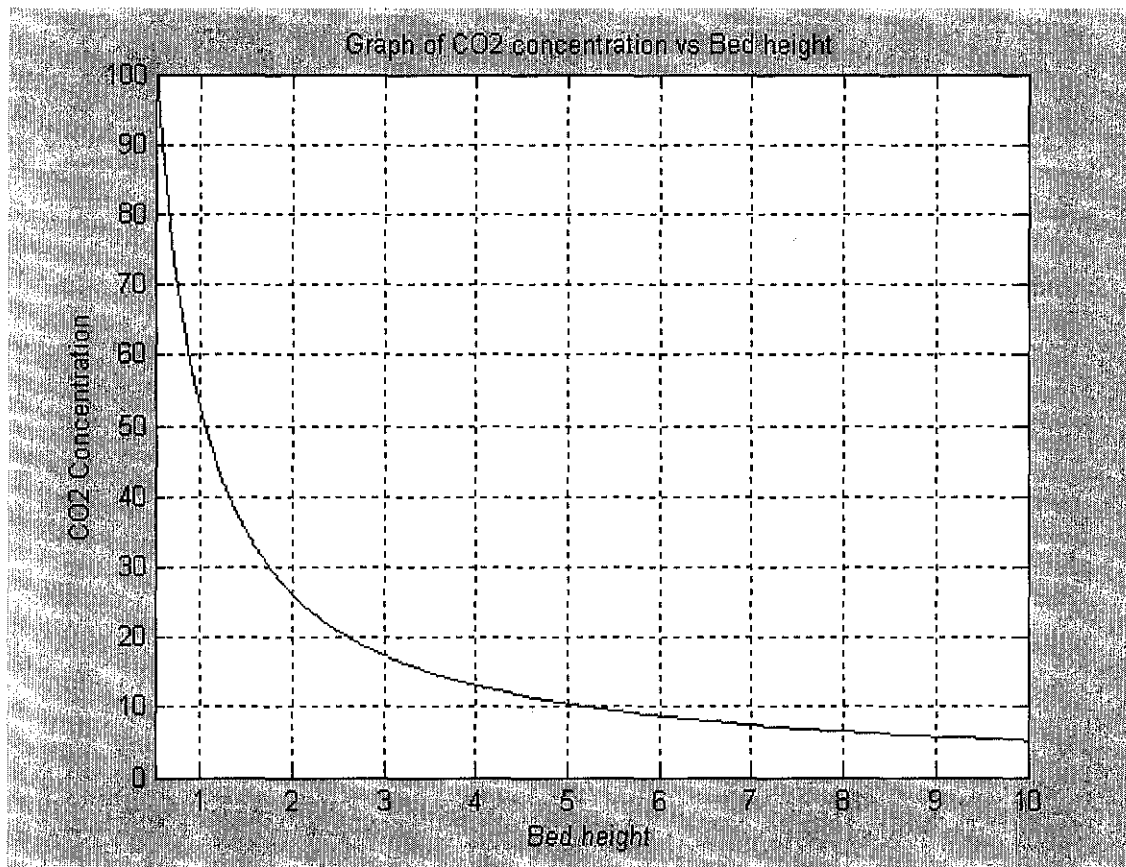


Figure 1. Graph of Carbon Dioxide versus Bed Height

4.4 Concentration Profile

Initially the catalytic activity of a carbon reforming of methane was predicted to be similar to partial oxidation or steam reforming of methane. However, it is observed that the carbon dioxide concentration decreases with the increasing height of catalyst bed. The reduction of the catalytic stability is much more in carbon dioxide reforming compared to the other two methods of methane reforming.

Carbon dioxide concentration decreases because of its reaction with methane to form carbon monoxide and hydrogen. The concentration also dropped at a very quick rate at the beginning and began to react slowly towards the end of the catalyst bed.

There are several reasons of why the concentration decreases quickly in the beginning and began to react slowly at halfway through the catalyst bed. One of them is the

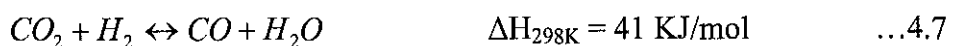
decrease in the reactant concentration. Initially the reactant concentration is high, contributing to large reaction rate along the earlier part of the catalyst bed. Further along the catalyst bed, reactant concentrations begin to drop causing the reaction rate to become lower.

Main reason for rapid reaction rate in the beginning and slow rate towards the end of the catalyst bed is because of catalyst deactivation. The dissociation of methane into carbon and hydrogen has resulted the carbon formation and deposits on the catalyst surface. The formation of carbons onto catalyst active site has decreased the catalytic activity by hindering of catalyst active site from the reactants particle.

Another reason for the decrease in reaction rate can be related to catalyst deactivation. Study shows that the catalyst starts to deactivate after 50 hours of operation [9]. The main reason for catalyst deactivation is the deposition of carbon onto catalyst surface as a result of methane dissociation into carbon and hydrogen. The deposition of carbon onto catalyst surface reduces the fraction of active site and prevents reactant from being attach to the active catalyst site, hence hinder further reaction.

At the beginning freshly reduced catalyst has no carbon deposit to block the reaction from occurring. However as the reaction occurs, carbon created from the methane deformation accumulates on the catalyst active site first because of its high adsorption properties. There will be at certain point where the carbon deposit will start to decrease the activity of the catalyst since large amount of reactants leaves the reactor without reacting.

Another reason for rapid concentration decay of the reactants may probably because of the reverse water-gas shift reaction (RWGS). [10]



This reaction is one of an elemental reaction that might occur during the carbon dioxide reforming. The reaction has caused the concentration of carbon dioxide to drop whereas it should dissociate into carbon monoxide and oxygen.

Formation of oxygen atom during reforming process can also decrease the catalyst activity. Oxidation of catalyst active site has caused the catalytic activity to drop since the some of the catalyst active sites have change into different material thus having different adsorption and desorption properties.

Catalytic activity can also drop because of inhibition effect. The slow desorption of product from the catalyst active site might occur thus hindering reactants from being adsorbed on the active site. This also occurs because of insufficient active site available since most of the active sites have been occupied with other reactant while some others have been blocked by carbon deposits.

There is also loss of catalyst material which contributes to the low catalytic activity after a certain period of the reaction. This loss is due to sintering effects where the dynamics of the catalyst beds become too rigorous causing a small volume of catalyst active sites to be destroyed.

The catalyst also suffers from sintering by presence of water particle in the RWGS reaction. Water particles initially will adsorb onto catalyst active site. Rapid heating of the reactor temperature will cause the water to evaporate at high rate thus damaging the catalyst structure. Some of the catalyst also experience carryover (entrainment) into downstream line of the process plant.

4.5 Validity of Assumption

Without all the assumptions made, there could be no possible way of achieving the result. All the assumptions made were applied to the Matlab model to imitate the real experimental situation.

In order to achieve the rate of reaction, it is assumed that the reaction occurs only at the external surface of a catalyst particle. This assumption was made since the size of catalyst particles is about $110\mu\text{m}$. The small size of catalyst particles will have smaller pores size hence restricting the entrance of reactant particles.

Since the reaction only occurs at the external surface of the catalyst particles, the diffusion terms in the reaction mechanism can be neglected. These assumptions were found to be true when the model was tested with larger catalyst particles. (The test will be discussed in later stages of this chapter).

In the test, the concentration profile was observed to drop at higher rate because of the presence of micropores. Bigger catalyst particles possess bigger micropores that can acquire more catalytic activity due to maximization of catalyst active site on the catalyst surfaces.

In the process of obtaining the design equation, the only assumption made was the simplification of the emulsion phase equation. This assumption was made due to the large ratio of bubble velocity to the minimum fluidized bed.

From the ratio of both bubble velocity and minimum fluidized velocity, it can be said that the reactor experiences mostly bubble phase rather than emulsion phase. In other words, the reaction occurs mainly in the bubble phase and only in a very small portion of the reactor, reaction occurs in the emulsion phase hence the emulsion part can be simplified.

Provided if the emulsion and the bubble phase have the same amount of volume in the fluidized reactor, the concentration profile might behave a little different. The concentration profile may probably differ from the one that has been proven in the experiment. The profile is expected to decrease at linear rate and at a slow pace. This is because less reaction to occur in the emulsion phase due to small reactant flow rate. The reactor also will need to add more height to the catalyst bed in order to achieve optimum yield.

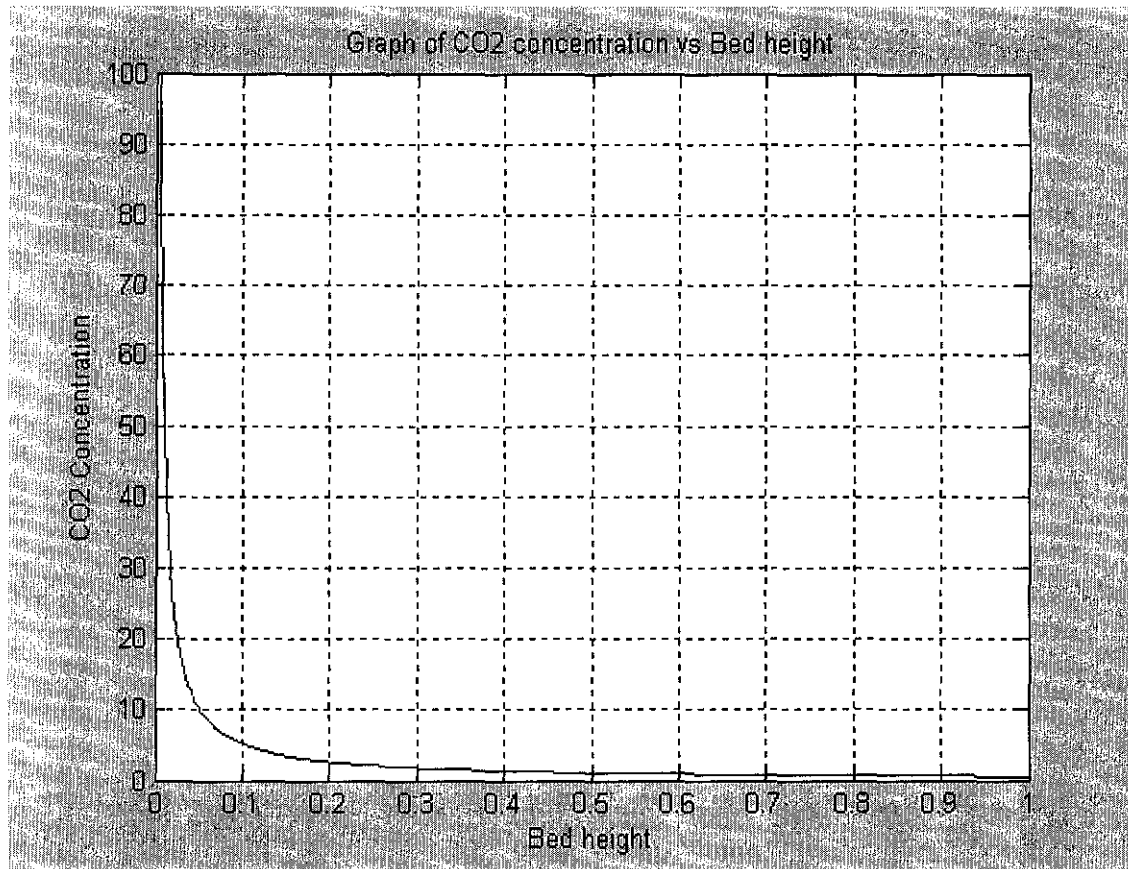


Figure 2: Graph for Carbon dioxide concentration versus bed height

4.6 Other Test

The model equation tested with bigger catalyst particle diameter. It is found that the concentration of carbon dioxide decrease at a faster rate compared to the previous one. Please refer figure 2. The bigger the catalyst might give better reaction rate since the reaction could also occur in the micropores of the catalyst. In the previous experiment,

the catalyst used was too small that the reaction occurs only at the external surface of the catalyst particle.

Larger size catalyst particle will have reaction at both external and internal surface. Larger catalyst particles will optimize more of its surface area since it can accommodate more active surface area. The only draw back of usage of bigger catalyst diameter is the big pressure drop across the fluidized bed reactor.

The previous experiment was using a catalyst particle diameter of $110\mu\text{m}$. this time the particle diameter was replaced with a bigger size, $\rho_s = 1 \text{ mm}$. The catalytic activity was observed to have a very high reaction rate in very short period of time. Suggested bed height for using the 1 mm diameter is 0.5 cm . This is because addition in catalyst bed would not have a significance conversion of the carbon dioxide.

There was another test that should have been conducted on the reaction model. However the test was not conducted because of time limitation. This test is to study the effect of the limiting reactants. If the concentration of the limiting reactant is to be increased, the product yield will increase. It is proposed that the effect of limiting reactant will give slight different in the concentration profile. Increment in limiting reactant will give higher conversion thus the final concentration of the reactant will be much less.

5 CONCLUSION

The modeling of the carbon dioxide reforming of methane can be said as successful. The objective of the modeling where it is constructed to study catalytic mechanism and activity has been achieved. The analyses of the concentration profile that have been acquired through the Matlab simulation have been discussed in the discussion part. However the model was not tested to its limit to maximize the outcome that might benefit the writer as well the reader.

There are some problems that have been encountered during the completion of this project. The main problem is time limitation. More time should have been allocated to do the project. Other problem is to find the information source that might assist in completing the subject. However, the writer was able to overcome the problem and came out with the final report of the project.

The study of kinetic analysis of a reaction should be continued as there are still more topics to cover. The reaction model should be given more time to test for different parameters and variables that might give new information regarding the reaction. A real laboratory experiment should be conducted based on the findings through the reaction model. Even it will cost a lot in buying all the equipments, it is the information that will benefit the whole society that counts.

6 REFERENCES

1. Robert H. Perry and Don W. Green, 1997, Perry's Chemical Engineer's Handbook 7th edition, McGraw-Hill International Editions.
2. Robert J. Farrauto and Calvin H. Bartholomew, 1997, Fundamentals of Industrial Catalytic Processes, Blackie Academic and Professional.
3. J.E. House, 1997, Principles of Chemical Kinetics, W.M.C. Brown Publishers
4. Charles N. Sattelfield, 1991, Heterogeneous Catalysis in Industrial Practice, 2nd edition, McGraw-Hill International Editions.
5. J.M. Smith, 1981, Chemical Engineering Kinetics, McGraw-Hill International Editions
6. Gilbert F. Froment and Kenneth B. Bischoff, 1990, Chemical Reactor Analysis and Design, 2nd edition Wiley Series in Chemical Engineering.
7. H. Scott Fogler, 1999, Element of Chemical Reaction Engineering, 3rd edition, Prentice hall
8. P. Harriot, J. C. Smith, W.L. Mc Gabe, 1982, Units operation of Chemical Engineering, 6th edition, McGraw Hill
9. T. Wurzel, S. Malcus and L. Mleczko, 16 November 1998, "Reaction Engineering investigations of CO₂ reforming in a fluidized bed" Chemical Engineering Science, 55 (18): 3955-3966
10. M. Souza, D. Aranda and M. Schmal, 5 July 2001, "Reforming of Methane with Carbon Dioxide over Pt/ZrO₂/Al₂O₃" Catalysis Today 21 (9517): 1-13
11. O. Takayasu, F. Sato, K. Ota and T. Hitomi, 1997, "Separate Production of Hydrogen and Carbon Monoxide by Carbon Dioxide reforming of Methane" Energy Convers. Mgmt 38 (96) 391-396
12. V. Tsipouriari, X. Verykios, 1998, "Kinetic study of the catalytic reforming of methane with carbon dioxide to synthesis gas over Ni/La₂O₃ catalyst" Catalysis Today 64 (2001): 83-90
13. A. Lemonidou, I Vasalos, 25 June 2001, "Carbon dioxide reforming of methane over 5 wt% Ni/CaO-Al₂O₃ catalyst" Applied Catalyst 228 (2002) 227-235

14. M. Matsukata, T. Matsushita and K. Euyama, 1996, " A novel Hydrogen/syngas production process: catalytic activity and stability of Ni/SiO₂" Chemical Engineering science 51 (11): 2769-2774
15. L. Mleczko, T Osrowski and T. Wurzel, 1996, "A fluidized-bed membrane reactor for the catalytic partial oxidation of methane to synthesis gas" Chemical Engineering Science 51 (11) 3187-3192
16. I. Rusu and Jean-Marie Cormier, 20 December 2001, " On a possible mechanism of the methane steam reforming in a gliding arc reactor" Chemical Engineering Journal 4021 (2002) 1-9
17. S.E Park, S. Nam, J. Choi and W. Lee, 1995, "Catalytic reduction of carbon Dioxide-the effects of catalysts and reductants" Energy Convers Mgmt 36 (69): 573-576

APPENDICES

Gantt Chart for Final Year Project

Week Number	1	2	3	4	5	6	7	8	9	10	11	12	13	14
Selection of Project Topic														
Propose topic	■	■												
Topic assigned to student		●												
Preliminary Research Work														
Literature review		■	■	■	■	■	■	■	■	■	■	■		
Data Compilation			■	■	■	■	■	■	■	■	■	■		
Submission of Preliminary Report					●									
Reaction Rate Analysis														
Data analysis					■	■	■	■	■	■	■	■		
Rate expression					■	■	■	■	■	■	■	■		
Submission of Progress Report								●						
Development of design expression							■	■	■	■	■	■		
EDX exhibition											●			
Simulation of Reaction										■	■	■	■	■
Submission of Interim Report														●

Completed
Milestone





Reaction engineering investigations of CO₂ reforming in a fluidized-bed reactor[☆]

T. Wurzel¹, S. Malcus², L. Mleczko^{*,3}

Lehrstuhl für Technische Chemie, Ruhr-Universität Bochum, D-44780 Bochum, Germany

Received 16 November 1998; accepted 21 July 1999

Abstract

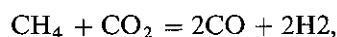
O₂ reforming of methane to synthesis gas over an Ni (1 wt%)/ α -Al₂O₃ catalyst was studied in lab-scale fluidized-bed reactors (d = 3.5 cm). In the whole range of reaction conditions ($p_{\text{CH}_4} = p_{\text{CO}_2} = 25\text{--}45$ kPa, $p_{\text{N}_2} = 10\text{--}50$ kPa, $T_R = 700\text{--}800^\circ\text{C}$, $u = 3.4\text{--}5$ cm, $m_{\text{cat}}/\dot{V} = 2.8\text{--}7.3$ g s ml⁻¹, $u/u_{mf} = 6.5\text{--}11.8$) a stable isothermal operation was achieved. The catalytic performance strongly depended on the oxidation state of the catalyst. When applying a reduced catalyst initial yields of carbon monoxide and hydrogen near the thermodynamic equilibrium were obtained. However, a slow decrease of methane conversion and syngas yield led by carbon deposition was observed. The fresh unreduced catalyst exhibited significantly lower activity. The in situ reduced catalyst was more active but yielded CH₄ and CO₂ conversions lower than predicted by the thermodynamic equilibrium. The reaction was not influenced by interphase gas exchange. Based on these results, reaction engineering modeling and simulation yielded a global kinetic model which described the experimental data with an error of less than 10% was developed. © 2000 Elsevier Science B.V. All rights reserved.

Keywords: CO₂-reforming; synthesis gas; fluidized-bed modeling

Introduction

In recent years, considerable attention has been paid to methane which is the main component of natural gas feedstock for the chemical and petrochemical industry. The indirect route via synthesis gas (syngas) remains the main way to convert natural gas into liquid fuels, ethanol, ammonia or oxygenates. Currently, syngas is mainly produced by steam reforming of methane (Adris, Lim, Lim & Grace, 1996; Qin, Lapszewicz & Jiang, 1994). However, the H₂ : CO ratio of 3 : 1 obtained by

steam reforming is higher than that needed for Fischer-Tropsch or methanol synthesis. In turn, further gas make up is necessary in order to obtain syngas which meets the requirements of the down-stream technologies.



$$\Delta_R H_{298\text{K}}^\circ = +247.9 \text{ kJ/mol.} \quad (1)$$

Lately carbon dioxide reforming of methane (see Eq. (1)) has gained increasing interest as an alternative process to produce syngas (Edwards, 1995). This process yields the low H₂ : CO ratio of 1 : 1 which is desirable for synthesis of oxygenated chemicals. CO₂ reforming can also be used for producing high-purity CO (Teuner, 1985; Kurz & Teuner, 1990). Furthermore, this reaction is of environmental significance since it consumes two molecules which contribute significantly to the greenhouse effect (Rostrup-Nielsen, 1994). Finally due to the high endothermicity of the reaction it can be used for the chemical energy storage (Wang, Lu & Millar, 1996; Gadalla & Sommer, 1989). Carbon dioxide reforming still has no commercial application by itself (Edwards & Maitra, 1994) but it is used in mixed reforming processes to reduce the H₂ : CO ratio (Teuner, 1987).

This paper is dedicated to Prof. Manfred Baerns on the occasion of his 70th birthday.

Present address: Lurgi Öl Gas Chemie GmbH, Frankfurt/Main, Germany.

Present address: University of New Brunswick, Fredericton, Canada.

Present address: Bayer AG, ZT-TE 4.4, Geb.E41, D-51368 Leverkusen, Germany.

Corresponding author. Tel.: +49-234-700-4102; fax: +49-234-4115.

E-mail address: l.mleczko@risc.techem.ruhr-uni-bochum.de (L. Mleczko).

nomenclature

	cross-sectional area of reactor, m^2	N_{orif}	number of distributor holes, dimensionless
j,i	concentration of component i in the j^{th} segment of the bubble phase, mol m^{-3}	NR	number of reactions dimensionless
j,i	concentration of component i in the j^{th} segment of the emulsion phase, mol m^{-3}	m_{cat}	mass of catalyst, g
o	initial bubble diameter, m	η_g	gas viscosity, Pa s^{-1}
j	local bubble diameter in j^{th} segment, m	p	partial pressure, kPa
	particle diameter, μm , m	$Q_{p,l}$	reaction quotient of reaction l ($Q_{p,l} = \prod p_{i,j}^{\nu_{i,l}}$, var.
H_{298K}^0	standard reaction enthalpy, kJ mol^{-1}	r	reaction rate, $\text{mol s}^{-1} \text{kg}_{\text{cat}}^{-1}$
	porosity at minimum fluidization condition, dimensionless	$r_{B,j,l}$	rate of reaction l in the j^{th} segment of bubble phase, $\text{mol s}^{-1} \text{kg}_{\text{cat}}^{-1}$
j	local bubble hold-up in the j^{th} segment, dimensionless	$r_{E,j,l}$	rate of reaction l in j^{th} segment of emulsion phase, $\text{mol s}^{-1} \text{kg}_{\text{cat}}^{-1}$
	earth acceleration, m s^{-2}	ρ_{cat}	catalyst density, kg m^{-3}
	inner diameter, cm	ρ_g	gas density, kg m^{-3}
	measuring height, cm	ρ_P	particle density, kg m^{-3}
	height, cm	STP	standard conditions, dimensionless
	component, dimensionless	t	time, min, h
	segment number in the fluidized bed, dimensionless	T	temperature, $^{\circ}\text{C}$
	adsorption constant of component i , atm^{-1}	T_R	reaction temperature, $^{\circ}\text{C}$
i,l	thermodynamic equilibrium constant of reaction l , var.	TOS	time on stream, h
	kinetic constant of reaction l , var.	u	superficial gas velocity, cm s^{-1}
E,i	mass transfer coefficient in the j^{th} segment, s^{-1}	u_j	superficial gas velocity in the j^{th} segment, cm s^{-1}
	reaction number, dimensionless	u/u_{mf}	fluidization number, dimensionless
	average life time of a bubble, s	$u_{B,j}$	bubble rise velocity in the j^{th} segment, m s^{-1}
at	mass of catalyst, g	$\nu_{i,l}$	stoichiometric coefficient of component i in reaction l , dimensionless
	at minimum fluidization condition, dimensionless	\dot{V}	volume flow, $\text{m}^3 \text{s}^{-1}$
li	mass of nickel, g	$V_{B,j}$	volume of bubble phase in the j^{th} segment, m^3
mv, BE, i, j	convective flow of component between bubble and emulsion phase in the j^{th} segment of the fluidized bed due to increase of total numbers of moles, mol s^{-1}	$V_{CP,j}$	volume of cloud phase in j^{th} segment, m^3
		$V_{EP,j}$	volume of emulsion phase in j^{th} segment, m^3
		X_i	conversion of component i , %
		X_i^0	initial conversion of component i , %
		Y_i	yield of component i , %

against this background numerous works dealing with the investigation of CO_2 reforming in fixed-bed reactors over supported metal catalysts were reported (for a review see Wang et al., 1996). The reaction temperatures applied in these investigations ranged from $^{\circ}\text{C}$ (Masai, Kado, Miyako, Nishiyama & Tsuruya, 1988; Erdöhelyi, Cserenyi & Solymosi, 1993) up to $^{\circ}\text{C}$ (Yu, Choi, Rosynek & Lunsford, 1993). Among several transition metals which were proposed as active components, nickel (e.g. Vernon, Green, Cheetham & Ashcroft, 1992; Gadalla & Sommer, 1989), platinum (Masai et al., 1988; Vernon et al., 1992; Solymosi, Tsan & Erdöhelyi, 1991) and rhodium (e.g. Erdöhelyi

et al., 1993; Richardson & Paripatyadar, 1990) have found widest research interest. For several of these catalysts yields of CO and H_2 near the thermodynamic equilibrium were reported (e.g. Vernon, Ashcroft & Cheetham, 1991; Richardson & Paripatyadar, 1990). However, catalyst deactivation due to carbon deposition occurred. This deposition limited application of a fixed-bed reactor for this reaction (Rostrup-Nielsen & Bak Hansen, 1993; Seshan, ten Barge, Hally, van Keulen & Ross, 1994; Swaan, Kroll, Martin & Mirodatos, 1994; Au, Hu & Wan, 1994). Furthermore, in this reactor type steep temperature gradients caused by the high endothermicity of the reaction occurred. These, in turn, promoted

bon deposition (Rostrup-Nielsen & Bak Hansen, 1993; Zhang & Verykios, 1994).

In order to eliminate these obstacles which impede the commercialization of the title reaction the application of a fluidized-bed reactor was proposed (e.g. Olsbye, Wurzel & Mleczko, 1997). Excellent heat dissipation originating from the solids mixing in this reactor type can be utilized to obtain good temperature control in isothermal operation. Application of small particles should allow to overcome the intra-particle mass transfer limitation which seriously reduces catalyst efficiency in fixed beds (Adris et al., 1996). Until now, only few experimental studies have dealt with the performance of a fluidized-bed reactor for CO_2 reforming (Mirzabekova, Mamedov, Aliev & Krylov, 1992; Blom, Dahl, Salgtern, Sortland, Spjelvik & Tangstad, 1994; Olsbye et al., 1997). The reported results show that conversions near thermodynamic equilibrium can be attained although catalyst deactivation has not been prevented (Blom et al., 1994). These studies aimed mainly at catalyst testing with respect to their catalytic and mechanical stability.

Against this background reaction engineering investigations of CO_2 reforming over an $\text{Ni}/\alpha\text{-Al}_2\text{O}_3$ in a laboratory-scale fluidized-bed reactor were carried out. The work aimed at the optimization of reaction conditions for obtaining high syngas yields as a base for the determination of kinetic parameters. Special attention was paid to the influence of hydrodynamic and reaction conditions on the deactivation of the catalyst.

Method of investigation

1. Experimental

1.1. Catalyst

The Ni (1 wt%)/ $\alpha\text{-Al}_2\text{O}_3$ catalyst was prepared by the impregnation wetness technique from $\alpha\text{-Al}_2\text{O}_3$ (Janssen) with an aqueous solution of $\text{Ni}(\text{NO}_3)_2 \cdot 6\text{H}_2\text{O}$ (Merck). After drying for 12 h at 100°C the catalyst precursor was calcined in air at 470°C for 10 h. Particle diameters in the range 71–160 μm were used. The experimentally determined minimum fluidization velocity using nitrogen as the fluidizing gas amounted to $u_{\text{mf},800^\circ\text{C}} = 0.006$ m/s.

1.2. Catalyst characterization

The fresh unreduced as well as samples of $\text{Ni}/\text{Al}_2\text{O}_3$ catalyst used in different series of experiments were characterized by applying several surface and bulk techniques. Carbon deposits were determined by means of temperature programmed oxidation (TPO). X-ray diffraction (XRD) analysis was performed in order to determine the phase composition of the catalyst samples and to correlate the catalytic activity to specific phases. Transmission electron microscopy (TEM) analysis of different samples aimed at the visualization of nickel particles and carbon deposits.

2.1.3. Apparatus

Experiments were carried out at atmospheric pressure in two fluidized-bed reactors made of quartz with inner diameters of $\text{ID} = 3$ cm and 5 cm (see Fig. 1). In the preheating section ($L = 80$ cm, $\text{ID} = 2$ cm) the feed gas was warmed up to 400°C before distributing through a porous quartz plate ($d_{\text{pore}} = 40\text{--}90$ μm). The bed temperature was controlled by heating the catalytic section from outside. In order to reduce particle entrainment a disengaging section and an internal cyclone were located at the top of the reaction zone.

For measuring the bed temperature, thermocouples within a quartz tube were located in three axial positions of the fluidized bed. Reactants (CH_4 , CO_2 and N_2 serving as internal standard) and products (H_2 and CO) were analyzed by on-line gas chromatography. The amount of water which was condensed downstream from the reactor was calculated from the oxygen balance. Concentration profiles were measured applying an axial movable sample tube ($\text{OD} = 0.8$ cm). A detailed description of the experimental equipment is given elsewhere (Mleczko, Pannek, Rothaemel & Baerns, 1996a).

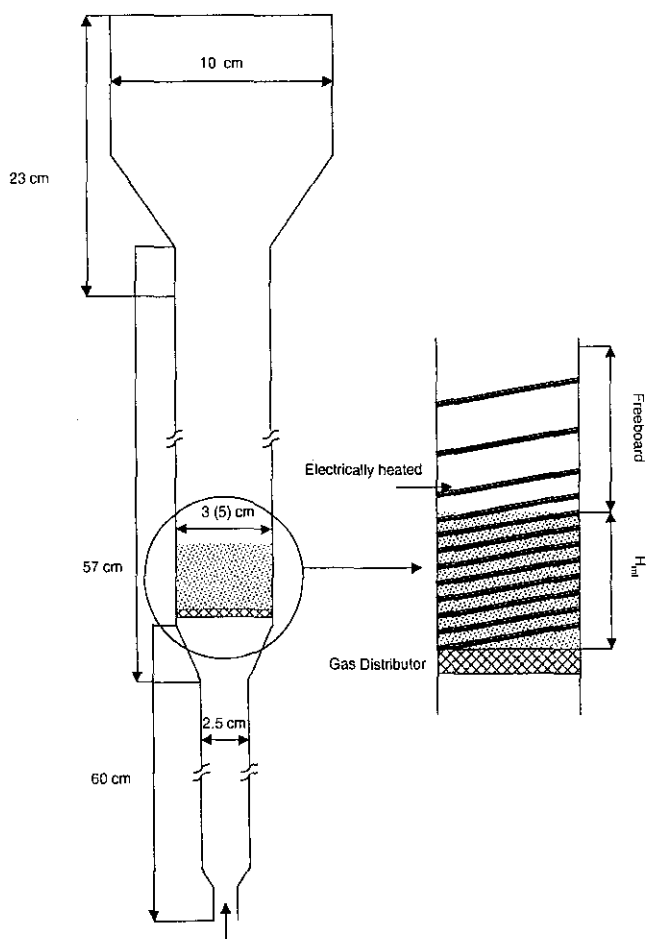


Fig. 1. Schematic sketch of the fluidized-bed reactor applied.

4. Experimental conditions

In all experiments a CH₄:CO₂ ratio of 1:1 was used. Nitrogen-dilution was varied between 10 and 20 Pa. The reaction was investigated between 700 and 800 °C. The reactor was operated in the bubbling regime (u_{mf} = 6.5–11.8). Catalyst mass was varied between 106 and 177 g. The other experimental conditions are given in the following part.

Modeling

1. Reactor model

The hydrodynamics of a fluidized bed was described by a model that originated from the bubble assemblage model of Kato and Wen (1969). In this model the fluidized bed is divided into segments. The height of the segments corresponds to the local bubble diameter. The model is based on the two-phase theory of fluidization. According to this theory, the bed is divided into two phases, i.e. the emulsion phase and the bubble phase. Between the phases exchange of gas takes place; the interphase gas exchange coefficient was calculated from the correlation of Kobayashi and Arai (1967). Through the emulsion gas flows with the minimum fluidization velocity which was calculated from the correlation of Wen and Yu (1966). The excess gas flows in the form of bubbles. The bubble phase consists of particle-free bubbles that are surrounded by cloud and wake. The cloud and wake have the same porosity as the emulsion phase and travel together with bubbles. For describing the dynamics of bubbles, i.e. bubble diameter and velocity the correlation of Werther (1992) was used. The correlation of Werther describes growth of bubbles as a result of coalescence and splitting. However, during the reforming reaction local bubble diameter, superficial gas velocity and the interphase gas exchange are also influenced by the increase of gas volume due to chemical reaction. The

model equations are given below (Eqs. (2) and (3)). The correlations used for hydrodynamic modeling are summarized in Table 1 (refer also Mleczko, Ostrowski & Wurzel, 1996b; Wurzel & Mleczko, 1998).

Model equation for emulsion phase:

$$A_T u_{mf} [c_{E,i,j-1} - c_{E,i,j}] + k_{BE,j} V_{B,j} [c_{B,i,j} - c_{E,i,j}] + \sum_{i=1}^{NR} v_{i,i} r_{E,j,i} (1 - \epsilon_{mf}) \rho_{cat} V_{EP,j} - n_{conv,BE,i,j} = 0 \quad (2)$$

Model equation for bubble phase

$$A_T (u_j - u_{mf}) [c_{B,i,j-1} - c_{B,i,j}] - k_{BE,j} V_{B,j} [c_{B,i,j} - c_{E,i,j}] + \sum_{i=1}^{NR} v_{i,i} r_{B,j,i} (1 - \epsilon_{mf}) \rho_{cat} V_{CP,j} + n_{conv,BE,i,j} = 0 \quad (3)$$

2.2.2. Rate equation and estimation of kinetic parameters

Reaction rate of CO₂ reforming was calculated using a Langmuir–Hinshelwood rate expression. Because water–gas-shift reaction takes place simultaneously during CO₂ reforming (Olsbye et al., 1997) this reaction was also taken into account to describe the experimental results. Reaction rate of the water–gas-shift reaction was calculated by applying first-order rate equation. For both reactions vanishing reaction rates when approaching equilibrium were taken into account (see Eqs. (4) and (5)). These rate equations were already applied for describing kinetics of dry reforming of methane over the Ni/La/Al₂O₃ catalyst (Olsbye et al., 1997).

$$r_{CO_2 - Ref} = \frac{k_{CO_2 - Ref} p_{CH_4} p_{CO_2}}{(1 + K_1 p_{CH_4} + K_2 p_{CO}) (1 + K_3 p_{CO_2})} \times \left(1 - \frac{Q_{P,CO_2 - Ref}}{K_{P,CO_2 - Ref}} \right) \quad (4)$$

Table 1
Correlations used for the calculation of hydrodynamic parameters

Parameter	Correlation	Reference
u_{mf}	$u_{mf} = \eta_g \frac{(33.7^2 + 0.0408 d_p^3 \rho_g (\rho_p - \rho_g) \eta_g^{-2})^{1/2} - 33.7}{(\rho_g d_p)}$	Wen and Yu (1966)
$k_{BE,j}$	$k_{BE,j} = 0.11/d_{B,j}$	Kobayashi and Arai (1967)
$d_{B,0}$	$d_{B,0} = 1.3 [(A_T u_0 (N_{orif} A_T)^{-1})^2 g^{-1}]^{0.2}$	Werther, 1992
$\frac{d}{dh} d_{B,j}$	$\frac{d}{dh} d_{B,j} = \left(\frac{2 \epsilon_{B,j}}{9 \pi} \right)^{1/3} - \frac{d_{B,j}}{3 \lambda u_{B,j}}$	Werther (1992)
$\epsilon_{B,j}$	$\epsilon_{B,j} = 0.8 (u_j - u_{mf}) / u_{B,j}$	Werther (1992)
λ_B	$\lambda_B = 280 u_{mf} / g$	Werther (1992)
$u_{B,j}$	$u_{B,j} = 0.8 (u_j - u_{mf}) + 0.71 \times 3.2 \sqrt{g d_{B,j}}$	Werther (1992)

le 2

quency coefficients estimated for CO₂-reforming and water-gas-shift reaction and adsorption constants adapted from Olsbye et al. (1997)

Reaction	k_0 (mol s ⁻¹ g _{cat} atm ⁻²)	K_1 (atm ⁻¹)	K_2 (atm ⁻¹)	K_3 (atm ⁻¹)
CH ₄ reforming	0.0150 ± 0.0039	0.52	10	27
Water-gas-shift reaction	0.0120 ± 0.0041			

$$r_{\text{CH}_4} = k_{\text{WGS}} P_{\text{CO}_2} P_{\text{H}_2} \left(1 - \frac{Q_{\text{P,WGS}}}{K_{\text{P,WGS}}} \right) \quad (5)$$

kinetic parameters were determined by comparing model predictions (using the aforementioned reactor model) with the experimental data reported in this paper. Adsorption constants were adapted from Olsbye et al. (1997) (see Table 2). For the non-linear parameter optimization a random search method was applied. In this routine the goal function was built as the sum of squares of differences between measured and predicted conversions of methane and carbon dioxide. The details of the optimization routine are presented elsewhere (Wurzel, Mleczko & Baerns, 1997).

Results and discussion

Reactor operation and catalytic performance

1. Reactor operation

The Ni/α-Al₂O₃ catalyst was mechanically stable and fully fluidizable in the whole range of the investigated reaction conditions. From the bed with the height of 7 cm ($m_{\text{cat}} = 177.2$ g) during 129 h on stream 5.3 g catalyst was lost; the average rate of entrainment amounted 0.041 g h⁻¹. The good fluidizability of the catalyst resulted in a good temperature control (see Fig. 2). The fluidized bed zone showed isothermal behavior. However, in the grid zone (0–1 cm) a temperature gradient up to 30 K occurred. The temperature drop in the distribution zone was significantly higher than the one measured in the same reactor for the oxidative coupling of methane (Mleczko et al., 1996a) and for the catalytic partial oxidation of methane to syngas (POX) (Mleczko & Wurzel, 1997). This indicates that the temperature drop is not only caused by the cold inlet gases but also by the high exothermicity of the reforming reaction. In the freeboard the temperature increased up to 825°C since this part of the reactor was still heated.

2. Catalytic performance

Highest conversions and syngas yields were achieved under the following reaction conditions: $T_R = 800^\circ\text{C}$, $f = 5$ cm, $u/u_{mf} = 11.8$, $m_{\text{cat}}/\dot{V}_{\text{STP}} = 4.7$ g s ml⁻¹, $p_{\text{CH}_4} : p_{\text{CO}_2} : p_{\text{N}_2} = 1 : 1 : 2$. Methane and carbon dioxide

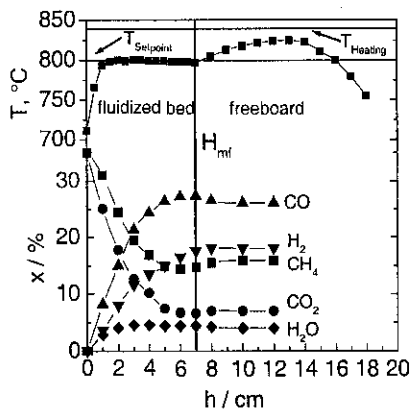


Fig. 2. Axial temperature as well as axial concentration profiles of reactant (CH₄, CO₂) and product (CO, H₂, H₂O) components concentration profile (CH₄ : CO₂ : N₂ = 1 : 1 : 0.86, $u/u_{mf} = 8.6$, $H_{mf} = 7$ cm, $T_R = 800^\circ\text{C}$).

conversion amounted to 90 and 93%, respectively. Hydrogen and carbon monoxide yield amounted to 81 and 90%, respectively; this corresponds to a H₂ : CO ratio of 0.9.

These results are in line with the published data. In almost all studies conversions near the thermodynamic equilibrium were achieved. No difference between fluidized and fixed beds could be recognized. A comparison between conversions and yields obtained in this work and those reported in the literature is difficult due to the differences between reaction conditions and loading of the catalyst with an active component. In order to overcome this obstacle the activity of the investigated catalyst was compared with other systems on the basis of the mass of the active component. This approach is justified by the linear dependency of the catalyst activity on the Ni loading (Goetsch, Say, Vargas & Eberly, 1989). The contact times reported for fixed beds were shorter than the one applied in this work ($m_{\text{Ni}}/\dot{V}_{\text{STP}} = 0.047$ g s ml⁻¹). Although the contact times for achieving thermodynamic equilibrium are comparable with those reported in the literature, the activity of the catalyst applied in this work was significantly lower than that of the catalyst prepared by SINTEF (Blom et al., 1994). Finally it should be taken into account that the validity of the linear dependence of the catalytic activity on the Ni loading is limited, e.g. for Ni/NaY-zeolite catalysts the activity passed

ough a maximum with increasing nickel loading (Lang et al., 1996).

Since it is generally accepted that reforming reactions are the rate-determining steps during partial oxidation of methane to syngas a comparison between CO_2 reforming and partial oxidation in fluidized beds can be made. When performing POx over various supported nickel catalysts methane conversions close to the thermodynamic equilibrium were achieved at significantly shorter contact times than in this work (Bharadwaj & Schmidt, 1994; Olsbye, Tangstad & Dahl, 1994; Mleczko & Wurzel, 1997; Santos, Menendez, Monzon, Santamaria, Miro Lombardo, 1996). The fact that CO_2 reforming itself is faster than when it is performed during partial oxidation conditions was already stated in other works (e.g. Peters, Dolf & Voetter, 1955; Lapszewicz & Xiang, 1992). This suggests that the reforming reactions are promoted when oxygen is present. In order to explain this effect it can be postulated that carbon deposits which limit the overall catalytic activity are burnt off easier with oxygen than with carbon dioxide. Furthermore, it is supposed that the methane pyrolysis which is assumed to be the rate-determining step of the reforming reactions can be accelerated since hydrogen is withdrawn from adsorbed methane by adsorbed oxygen.

Parameters influencing catalytic activity and stability

1. Activity of the fresh catalyst

In the fresh (not-pretreated) catalyst nickel is completely oxidized. Therefore, when measuring the initial activity of the catalyst the activity of the oxidized NiO is for CO_2 reforming can be determined. Furthermore, effect of in situ reduction on catalytic activity during reaction can be analyzed. Moreover, the influence of the reaction conditions on the catalyst state can be observed by determining the course of conversions over time on stream. In the experiment the methane-to-carbon dioxide ratio amounted to 1 : 1. The feed was diluted with nitrogen ($p_{\text{N}_2} = 30 \text{ kPa}$). The height of the settled bed and the fluidization number (u/u_{mf}) amounted to 5 cm ($m_{\text{cat}} = 1.2 \text{ g}$) and 8.6, respectively.

The fresh catalyst showed a very low activity for CO_2 reforming, e.g. the initial conversions of methane and carbon dioxide amounted to 9 and 13%, respectively (see Fig. 3). Under reaction conditions activity of the catalyst increased. The characterization of the catalyst surface indicated that these changes in the catalytic activity can be correlated with the oxidation state of Ni sites. XRD analysis showed that the fresh catalyst contained completely oxidized nickel (see Fig. 4a). The low initial conversions indicate that oxidized nickel sites exhibit low catalytic activity for CO_2 reforming. Therefore, slow continuous reduction of nickel sites by non converted methane resulted in the increase of conversion. This explanation is confirmed by XRD (see Fig. 4b) and TEM

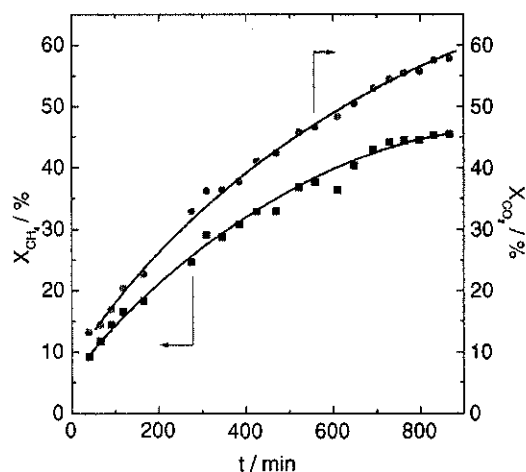


Fig. 3. Dependence of methane and carbon dioxide conversions on time on stream applying a fresh catalyst ($\text{CH}_4 : \text{CO}_2 : \text{N}_2 = 1 : 1 : 0.22$, $u/u_{mf} = 8.6$, $T_R = 800^\circ\text{C}$, $H_{mf} = 5 \text{ cm}$).

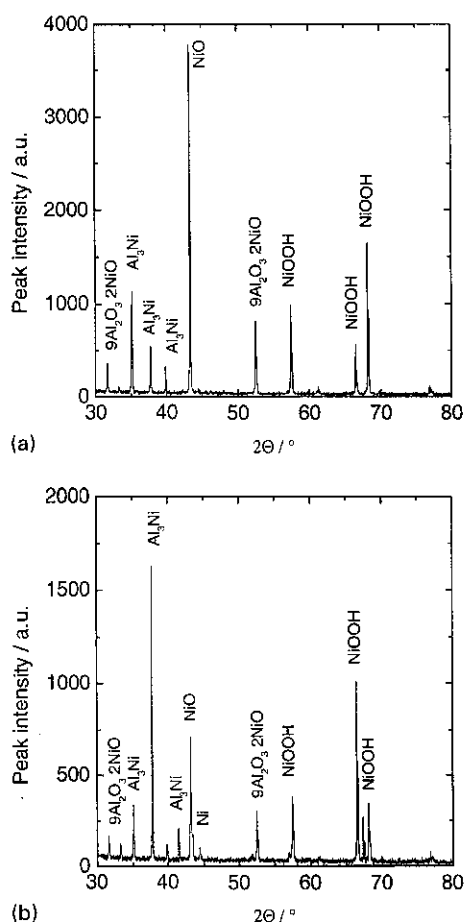


Fig. 4. XRD pattern of the fresh (unreduced) catalyst (a) and (b) of the catalyst used for CO_2 reforming after 120 h on stream ($\text{CH}_4 : \text{CO}_2 : \text{N}_2 = 1 : 1 : 2$, $u/u_{mf} = 11.8$, $H_{mf} = 5 \text{ cm}$, $T_R = 800^\circ\text{C}$).

analysis of the used catalysts (after 120 h on stream) which showed that during CO_2 reforming metallic Ni sites were formed. The reduction process is promoted by increasing conversion since the partial pressure of

hydrogen which is a more efficient reducing agent than methane increases during the activation period. The proposed explanation for the increase of the activity of fresh Al_2O_3 catalyst agrees well with published information; also other investigators reported that an increase of the reduction degree of supported metal catalysts (Ni) resulted in higher conversions when performing dry steam reforming (Au et al., 1994; Dissanayake, Synek, Kharas & Lunsford, 1991; Santos et al., 1996). After a period of 13 h the catalyst attained a stationary state; no further substantial changes in conversions of methane and carbon dioxide occurred. Final conversions, that amounted to 46% for methane and 58% for carbon dioxide were lower than those calculated for the thermodynamic equilibrium. In contrast to the results reported for the catalytic partial oxidation of methane to synthesis gas for which methane conversions near the thermodynamic equilibrium after an in situ activation of catalyst were achieved (e. g. Dissanayake et al., 1991; Santos et al., 1996), final conversions during CO_2 reforming were at comparable contact times significantly lower than those predicted by thermodynamics.

2. Catalyst deactivation

Catalytic stability was investigated by studying two catalysts applied for dry reforming over a period of 60 h that had exhibited different initial activities. Different catalytic activity was established by treating the first catalyst with O_2/N_2 (1 : 1) for 1 h at 600°C after 60 h on stream (CO_2 reforming). The second catalyst was not treated prior to reaction. The bed with the stationary height of 5 cm for the first catalyst and 3 cm for the second one was fluidized with a gas velocity of 7.1 cm s^{-1} ($u/u_{mf} = 11.8$). In both experiments the reaction temperature and the methane-to-carbon dioxide ratio amounted to 800°C and 1 : 1, respectively. The feeds were diluted with nitrogen ($p_{\text{N}_2} = 50 \text{ kPa}$). The experiments covered a period of approx. 100 h.

For both catalysts two periods can be recognized (see Fig. 5). In the first period the activity of the catalyst varied with TOS. In the second period both catalysts attained constant catalytic activity. The catalyst that had exhibited high initial activity ($X_{\text{CH}_4}^0 = 90\%$, $X_{\text{CO}_2}^0 = 86\%$) deactivated; after 50 h on stream conversions dropped to 78% for methane and 86% for carbon dioxide. Simultaneously, yields dropped from 82 to 75% for hydrogen and from 90 to 83% for carbon monoxide. TPO measurements performed for the $\text{Ni}/\text{Al}_2\text{O}_3$ catalyst (see Fig. 6) indicate that during CO_2 reforming continuous carbon deposition occurred, which is assumed to be possible for the loss of activity. After 8 h on stream only small amounts of carbon were deposited on the catalyst which could be burnt off at a temperature of around 680°C . In contrast, the specimen which was taken at the end of the reaction period (approx. 100 h) showed a substantial larger amount of carbon deposits which

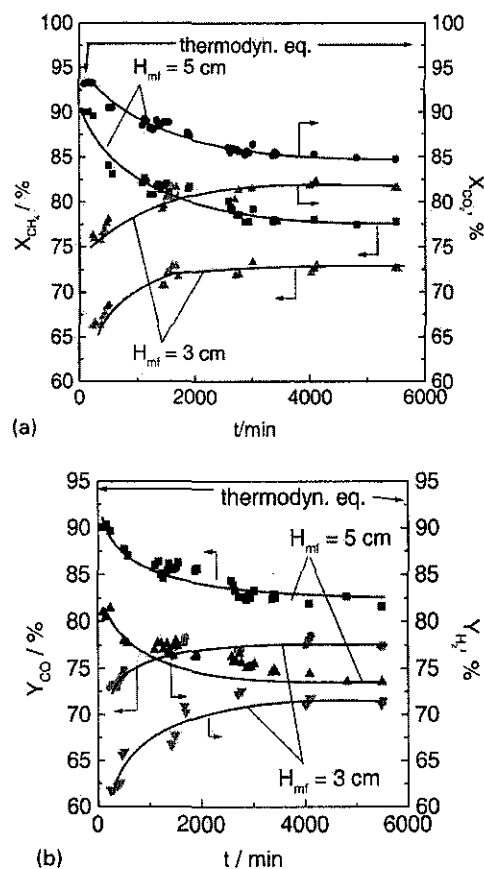


Fig. 5. Dependence of methane and carbon dioxide conversion (a) and (b) yield on time on stream for a regenerated ($H_{mf} = 5 \text{ cm}$) and a non-regenerated ($H_{mf} = 3 \text{ cm}$) catalyst ($\text{CH}_4 : \text{CO}_2 : \text{N}_2 = 1 : 1 : 2$, $u/u_{mf} = 11.8$, $T_R = 800^\circ\text{C}$).

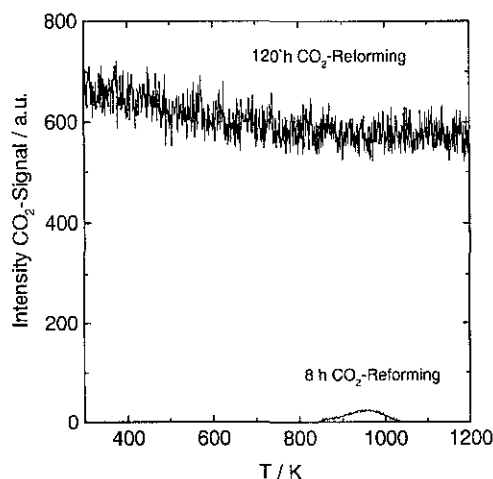


Fig. 6. Intensity of the CO_2 signal during TPO for two catalyst samples differing in time on stream ($\text{CH}_4 : \text{CO}_2 : \text{N}_2 = 1 : 1 : 2$, $u/u_{mf} = 11.8$, $H_{mf} = 5 \text{ cm}$, $T_R = 800^\circ\text{C}$).

could be burnt off continuously over the whole range of temperature. Furthermore, a second catalyst phase of black color was built up. The formation of the carbon deposits on the catalytic surface was also confirmed by

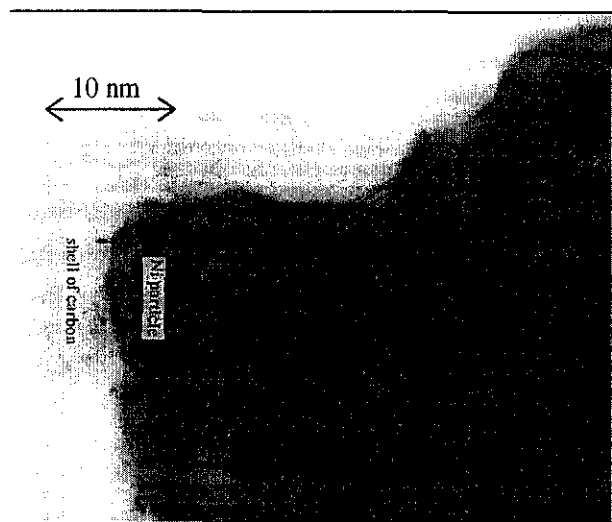


Fig. 7. TEM photography of the catalyst after 100 h of CO_2 reforming ($\text{CH}_4 : \text{CO}_2 : \text{N}_2 = 1 : 1 : 2$, $u/u_{mf} = 11.8$, $H_{mf} = 5$ cm, $T_R = 800^\circ\text{C}$).

D and TEM measurements. Furthermore, TEM analysis indicates that a shell of carbon was built up around nickel crystallites (see Fig. 7). The blocking of active sites by carbon deposits as the reason for the loss of catalytic activity during CO_2 reforming was also postulated by other investigators (e.g. Rostrup-Nielsen & Bak Hansen, 1993; Bitter, Hally, Seshan, van Ommen & Lercher, 1996). The initial conversions and yields measured over the catalyst that exhibited low initial activity amounted to 10% for methane, 76% for carbon dioxide, 62% for hydrogen and 73% for carbon monoxide. For this catalyst, conversions and yields rose in the initial period with time on stream. Conversions increased to 73% for methane and 82% for carbon dioxide. Simultaneously, yields rose to 72% for hydrogen and 78% for carbon monoxide. The low initial activity of this catalyst charge is assumed to result from the passivation of deposited carbon during the off-stream period. The explanation that the aging of carbon deposits can be responsible for the decay of catalytic activity is supported by the work performed by Buyevskaya, Wolf & Baerns (1994) in the P reactor over an Rh catalyst. The initial increase of conversions and yields observed during the activation period can be attributed to the substitution of the passivated carbon by fresh, active carbon deposits during the reversed Boudouard reaction. When the passivated carbon was completely substituted by fresh carbon deposits a stationary state of constant catalytic activity was achieved.

The stationary state that was obtained after approximately 15 h independent of the initial catalyst state is attributed to a dynamic equilibrium between reactions that consume deposited carbon (reversed Boudouard reaction) and those that produce carbon deposits (methane pyrolysis). Due to continuous catalyst deactivation when performing CO_2

reforming in fixed-bed reactors (e.g. Swaan et al., 1994) and the steady-state activity in the fluidized-bed the conclusion is drawn that catalyst deactivation is influenced by the hydrodynamic conditions in the reactor type applied. In a fluidized-bed reactor deactivated catalyst particles are transported by means of the solid mixing into the carbon-dioxide-rich distributor zone where the carbon deposits can be consumed by the reversed Boudouard reaction. Therefore, a fluidized-bed reactor seems to be more suitable for performing CO_2 -reforming reaction than a fixed bed not only with respect to temperature control but also due to the slower deactivation of the catalyst. This is underlined by the different deactivation rates. For an Ni (6.2 wt%)/ Al_2O_3 - SiO_2 catalyst the deactivation rate in a fixed bed amounted to $3.7\% \text{ h}^{-1}$ (Swaan et al., 1994) whereas it amounted to $1.5\% \text{ h}^{-1}$ (Blom et al., 1994) and $0.6\% \text{ h}^{-1}$ (this work) in the fluidized bed.

3.2.3. Effect of water on catalyst regeneration

Since an excess of steam is known to prevent carbon deposition during the steam-reforming process experiments were conducted in which the catalytic activity with and without steam addition ($p_{\text{H}_2\text{O}} = 15$ kPa) was investigated. In these experiments the deactivated catalyst that exhibited low initial activity was used. The methane-to-carbon dioxide ratio was held constant at 1 ($p_{\text{CH}_4} = p_{\text{CO}_2} = 35$ kPa). Nitrogen dilution amounted to 15 and 30 kPa, respectively. The reforming reaction was carried out at 800°C in a catalytic bed ($H_{mf} = 5$ cm, $m_{\text{cat}} = 64$ g) fluidized with a gas velocity $u = 5.2$ cm s^{-1} ($u/u_{mf} = 8.6$).

For both investigated feed-gas compositions a similar dependence of catalytic activity on TOS was observed; in the first 15 h methane and carbon dioxide conversion increased followed by constant activity (see Fig. 8). Water in the feed had no effect on the period of activation. However, slightly lower conversions were measured when applying the dry feed due to thermodynamic

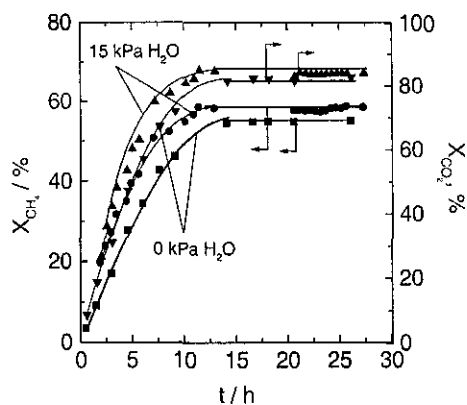


Fig. 8. Dependence of methane conversion on time on stream with and without water addition ($\text{CH}_4 : \text{CO}_2 : \text{N}_2 = 1 : 1 : 0.86$, $u/u_{mf} = 8.6$, $H_{mf} = 5$ cm, $T_R = 800^\circ\text{C}$).

isons. The addition of water to the feedstock also had significant influence on the catalytic stability of the γ - Al_2O_3 catalyst. This behavior can be explained by the stronger oxidation potential of carbon dioxide compared to water. Since the catalyst is continuously transported in the carbon-dioxide-rich distributor zone, carbon gasification by carbon dioxide is dominant compared to water.

3.3. Concentration profiles

In order to elucidate the reaction pathway of CO_2 reforming in a fluidized bed, axial concentration profiles were measured. In these experiments the minimum bed height H_{mf} and the $p_{\text{CH}_4} : p_{\text{CO}_2}$ ratio amounted to 7 cm and 1 : 1, respectively. Measurements were performed in a bed fluidized with a gas velocity of $u = 5.2 \text{ cm s}^{-1}$ ($u_{mf} = 8.6$) carrying out the reaction at 800°C .

The measured concentration profiles are presented in Fig. 2. The most significant changes of the concentrations took place within the first two centimeters of the fluidized bed. In this region a decrease of the concentrations of the feed gases methane and carbon dioxide from 35% at the inlet to 24.3% for methane and 17.6% for carbon dioxide was observed. Simultaneously, the concentrations of the products hydrogen and carbon monoxide increased up to 11.4 and 14.8%, respectively. Also in the upper part of the bed, the concentrations of methane and carbon dioxide decreased continuously, whereas the concentrations of the selective products hydrogen and carbon monoxide increased. However, with increasing distance from the distributor the concentration gradients decreased. Water yielded a maximum of 4.4% at a bed height of 1 cm followed by a flat decline of 4% at the end of the bed. At the end of the bed a decay of carbon monoxide concentration and an increase of the concentrations of the feed gases methane and carbon dioxide were measured. In the freeboard (8–12 cm) no further changes in concentrations occurred although the temperature was through a maximum in this region. This indicates that the reaction is heterogeneously catalyzed whereas gas-phase reactions have no influence on the extent of reaction.

In the whole bed, concentration of carbon dioxide was lower than the methane concentration. Also the hydrogen concentration was always lower than that of carbon monoxide. This indicates that beside the CO_2 -reforming reaction the water-gas shift reaction also takes place which results in a H_2/CO ratio below 1. With respect to the reaction rates it can be expected that the one for the water-gas reaction is faster than the one for CO_2 -reforming reaction since even in the distributor zone where the highest reaction rates for CO_2 reforming occur the difference between the methane and carbon dioxide concentration is significant. Simultaneously, formation of water also takes place. The product distribution in the bed is also

influenced by the steam-reforming reaction. This would explain the axial increase of the H_2/CO ratio (0.42–0.68) since steam reforming produces more hydrogen than carbon monoxide. However, steam reforming has only a minor effect on the methane conversion.

The concentration profiles presented above differ significantly from those measured during partial oxidation of methane for which almost constant gas composition was attained in the distributor zone (Olsbye et al., 1994; Mleczko & Wurzel, 1997). It is therefore assumed that thermodynamic equilibrium for partial oxidation is reached significantly faster compared to CO_2 reforming. As mentioned earlier it is concluded that CO_2 reforming itself is slower compared to its reaction rate during partial oxidation.

3.4. Effect of reaction conditions on catalytic performance

3.4.1. Effect of temperature

Temperature dependence of conversion was studied between 700 and 800°C . The methane : carbon dioxide ratio in the feed gas and the height of the bed amounted to 1 : 1 and $H_{mf} = 3 \text{ cm}$ ($m_{\text{cat}} = 106 \text{ g}$). The partial pressure of nitrogen and the fluidization number amounted to 30 kPa and 7.5, respectively.

Upon increasing temperature from 700 to 800°C the conversions of methane and carbon dioxide rose from 29 to 77% and from 43 to 84% (see Fig. 9). Simultaneously, the yields of the selective products hydrogen and carbon monoxide increased from 25 to 73% for hydrogen and from 40 to 81% for carbon monoxide. In the investigated temperature range conversions and yields predicted by the thermodynamic equilibrium were not achieved. However, the deviations between experimental values and the ones predicted by thermodynamic equilibrium decreased with increasing temperature. At a temperature of 800°C these deviations amounted to 11% for X_{CO_2} and 17% for Y_{H_2} . Hydrogen selectivity also rose with increasing

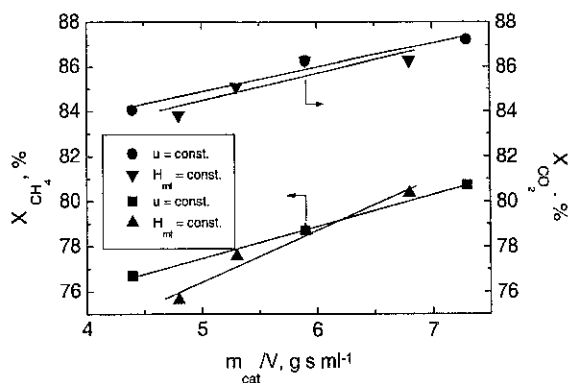


Fig. 9. Dependence of experimental (exp.) methane and carbon dioxide conversions and those predicted by thermodynamic equilibrium (eq.) on reaction temperature ($\text{CH}_4 : \text{CO}_2 : \text{N}_2 = 1 : 1 : 0.86$, $u/u_{mf} = 7.5$, $H_{mf} = 3 \text{ cm}$).

perature. These results indicate that the reaction is kinetically controlled in the investigated range of reaction conditions.

3.2. Effect of hydrodynamic conditions

In order to investigate the influence of hydrodynamic conditions on conversions and syngas yields contact times varied between 4.4 and 7.3 g s ml⁻¹ by changing the height of the bed and the gas velocity. Fluidization number was varied between 6.5 and 9.2 and the bed height between 3 and 5 cm (106.2–177.2 g cat.). Bed temperature and methane-to-carbon dioxide ratio at the reactor inlet amounted to 800°C and 1, respectively.

As expected the conversions of methane and carbon dioxide strongly depended on contact time (see Fig. 10). Monotonous growth of conversions and yields was achieved with increasing contact time. No significant difference between conversions was observed when increasing contact time by using higher beds or lower gas velocities. However, conversion was slightly less sensitive to changes of the contact time when this parameter was influenced by varying the mass of catalyst than when changing gas velocity. An increase of the contact time by reducing the fluidization number e.g. by changing gas velocity results in smaller bubbles. This, in turn, reduces the back-mixing of gas and improves mass transport between bubbles and the emulsion phase. Since the differences in the sensitivity of conversions to the changes of contact time did not differ significantly it can be concluded that in the investigated range of reaction conditions CO₂ reforming was not controlled by the inter-phase gas exchange.

The finding that the reactor performance is not controlled by mass transfer limitation is another difference to the partial oxidation of methane which confirms that the kinetics of both reactions are significantly different. How-

ever, with respect to large-scale application mass transfer limitation may become important. Simulations performed for catalytic partial oxidation (Wurzel & Mleczko, 1998) indicate that in an industrial-scale reactor the rate of reforming reactions was limited by the mass exchange between bubbles and the emulsion phase. In turn, longer contact times are required in order to achieve the same conversions as in the lab-scale reactor. This difference was explained by a significant change of the hydrodynamic conditions due to the formation of larger bubbles; in the lab-scale reactor bubble size amounted to approx. 0.5–1 cm (visually observed) whereas bubble diameters up to 20 cm were calculated for an industrial unit.

3.5. Simulation results

The conversions of methane measured in the stationary state were used for estimation of the frequency coefficients in the rate equations for the CO₂ reforming and water-gas-shift reaction. These conversions were compared with the ones by the previously presented model of the fluidized bed. In this approach the estimated kinetic parameters are biased by the uncertainty in the description of the bed hydrodynamics, i.e. the back-mixing and inter-phase gas exchange. Because studies of the effect of the contact time showed that the measured conversions were not limited by the inter-phase gas exchange this approach is justified. Additionally, the correlations used for prediction of the bubble dynamics were verified in cold-flow studies with the Ni/Al₂O₃ catalyst (Wurzel & Mleczko, 1998).

The estimated frequency coefficients and their confidence regions (based on a confidence number of 0.95) are presented in Table 2. With the developed model the measured conversions of methane and carbon dioxide could be reproduced with an error lower than 10% (see Fig. 11a). It has to be pointed out that all experimental data points were below those predicted by thermodynamics, i.e. the good accuracy of the model is not due to the thermodynamic limitations. The validity of the model was confirmed by good prediction not only of the integral data but also of the concentration profiles (see Fig. 11b). The concentrations calculated for the bubble and emulsion phase follow the experimentally measured concentrations. In line with the experimental findings that the inter-phase gas exchange in a lab-scale fluidized-bed reactor has only small influence on the conversions the calculated gas composition in the emulsion phase differed only slightly from the one in the bubble phase. Nevertheless, the better agreement of the values predicted for the bubble phase with the concentrations measured experimentally indicates that the predicted reaction rates are slightly underestimated. This conclusion is also in agreement with the results presented in the parity plot. Thus, this model can be used as

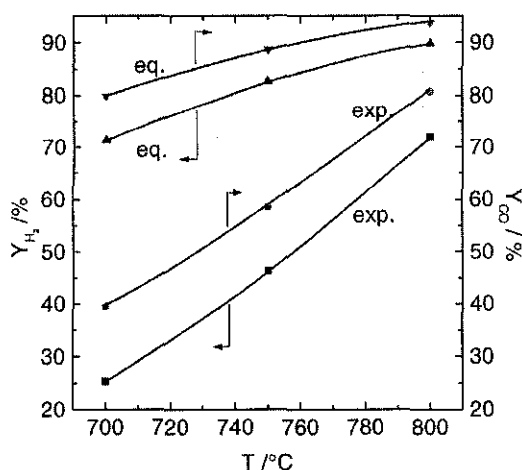
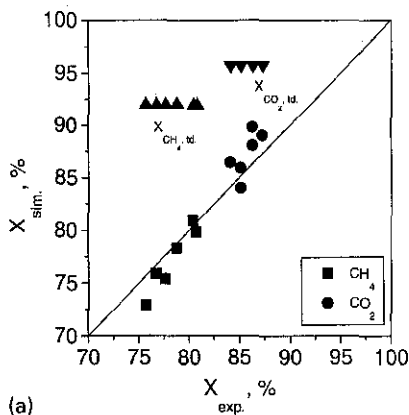
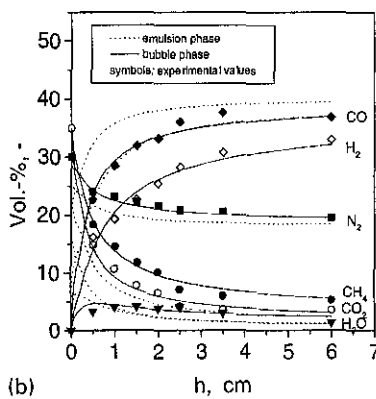


Fig. 10. Effect of hydrodynamic conditions on methane and carbon dioxide conversions ($\text{CH}_4 : \text{CO}_2 : \text{N}_2 = 1 : 1 : 0.86$, $T_R = 800^\circ\text{C}$, $u_{mf} = 6.5\text{--}9.2$, $H_{mf} = 3\text{--}5$ cm).



(a)



(b)

11. Parity plot of experimental and simulated methane and carbon dioxide conversion (a) and (b) measured and calculated concentration profiles (conditions see Fig. 2) during CO_2 reforming in a fluidized bed.

valuable tool for scaling-up of a fluidized-bed reactor dry reforming of methane.

Conclusions

Carbon dioxide reforming of methane was investigated a laboratory-scale (ID = 3, 5 cm) fluidized-bed reactor. The catalyst was well fluidizable and almost isothermal conditions were obtained over the whole range of reaction conditions studied. Highest conversions and gas yields were achieved applying the following reaction conditions: $T_R = 800^\circ\text{C}$, $H_{mf} = 5$ cm, $u/u_{mf} = 8$, $m_{cat}/\dot{V}_{STP} = 4.7$ g s ml⁻¹, $p_{\text{CH}_4} : p_{\text{CO}_2} : p_{\text{N}_2} = 1 : 1 : 2$. Methane and carbon dioxide conversion amounted to 90 and 93%, respectively. Hydrogen and carbon monoxide yield amounted to 81 and 90%, respectively; this corresponds to a $\text{H}_2 : \text{CO}$ ratio of 0.9. On the basis of experimental results a model of the fluidized-bed reactor for dry reforming of methane was developed. This model, that is able to reproduce experimental conversions with an error of less than 10% can be used as a valuable tool for reactor engineering studies of different reactor configurations proposed for the title reaction (see e.g. Młeczko, Malcus & Wurzel, 1997).

It has been shown that the performance of the Ni/ α - Al_2O_3 catalyst depended strongly on the oxidation state of the active component. Oxidized nickel sites showed a very low catalytic activity compared to the reduced, metallic ones; applying a reduced catalyst initial yields of carbon monoxide and hydrogen near the thermodynamic equilibrium were obtained, whereas the fresh unreduced catalyst exhibited significantly lower activity. With increasing time on stream a slow decrease of methane conversion and syngas yield was observed. Carbon deposition was found to be responsible for the deactivation of a highly active catalyst. After several hours on stream constant level of conversions and yields was achieved. This makes the significant difference in the deactivation behavior of the Ni/ Al_2O_3 catalyst in the fixed-bed and the fluidized-bed reactor. Addition of water to the feedstock showed no significant influence either on catalyst regeneration or on conversions.

The in situ reduced catalyst yielded CH_4 and CO_2 conversions lower than predicted by the thermodynamic equilibrium. CO_2 reforming in the laboratory reactor was not influenced by inter-phase gas exchange. This conclusion was also drawn from simulations of the lab-scale unit which resulted in a good reproduction of the experimental data. With respect to the process commercialization the fluidized-bed reactor seems to be a suitable reactor type. However, several serious problems like effect of pressure on the catalyst deactivation has to be investigated. Therefore, in the industrial-scale external catalyst regeneration might be necessary (Młeczko et al., 1997). Furthermore, the problem of metal dusting due to the high CO content in the reformed gas has to be taken into account with respect to the construction of the reformed gas boiler (Grabke, Krajak, Müller-Lorenz & Strauß, 1996; Hohmann, 1996).

References

- Adris, A. M., Pruden, B. B., Lim, C. J., & Grace, J. R. (1996). On the reported attempts to radically improve the performance of the methane steam reforming reactor. *Canadian Journal of Chemical Engineering*, 74, 177.
- Au, C. T., Hu, Y. H., & Wan, H. L. (1994). Pulse studies of CH_4 interaction with NiO/ Al_2O_3 catalysts. *Catalysis Letters*, 27, 199.
- Bharadwaj, S. S., & Schmidt, L. D. (1994). Syngas formation by catalytic oxidation of methane in fluidized bed reactors. *Journal of Catalysis*, 146, 11.
- Bitter, J. H., Hally, W., Seshan, K., van Ommen, J. G., & Lercher, J. A. (1996). The role of the oxidic support on the deactivation of Pt catalysts during the CO_2 reforming of methane. *Catalysis Today*, 29, 349.
- Blom, R., Dahl, I. M., Slagtern, A., Sortland, B., Spjelkavik, A., & Tangstad, E. (1994). Carbon dioxide reforming of methane over lanthanum-modified catalysts in a fluidized-bed reactor. *Catalysis Today*, 21, 535.
- Buevskaya, O. V., Wolf, D., & Baerns, M. (1994). Rhodium-catalyzed partial oxidation of methane to CO and H_2 . Transient studies on its mechanism. *Catalysis Letters*, 29, 249.

- anayake, D., Rosynek, M. P., Kharas, K. C. C., & Lunsford, J. H. (1991). Partial oxidation of methane to carbon monoxide and hydrogen over a Ni/Al₂O₃ catalyst. *Journal of Catalysis*, 132, 117.
- Ards, J. H., & Maitra, A. M. (1994). The reforming of methane with carbon dioxide - current status and future applications. *Studies in Surface Science Catalysis*, 81, 291.
- Ards, J. H. (1995). Potential sources of CO₂ and the options for its large-scale utilisation now and in the future. *Catalysis Today*, 23, 59.
- Erdöhelyi, A., Cserenyi, J., & Solymosi, F. (1993). Activation of CH₄ and its reaction with CO₂ over supported Rh catalysts. *Journal of Catalysis*, 141, 287.
- Evans, A. M., & Sommer, M. E. (1989). Carbon dioxide reforming of methane on nickel catalysts. *Chemical Engineering Science*, 44, 2825.
- Fischer, D.A., Say, G.R., Vargas, J.M., Eberly, P.E., 1989. Synthesis gas preparation and catalyst therefor. US Patent 4, 888, 131.
- Grover, H. J., Krajak, R., Müller-Lorenz, E. M., & Strauß, S. (1996). Metal dusting of nickel-base alloys. *Material Corrosion*, 47, 495.
- Hammann, F. W. (1996). Improve steam reformer performance. *Hydrocarbon Processing*, 75, 71.
- Hess, K., & Wen, C. Y. (1969). Bubble assemblage model for fluidized catalytic reactors. *Chemical engineering science*, 24, 1351.
- Ikeda, H., & Arai, F. (1967). Determination of gas cross-flow coefficient between the bubble and emulsion phases by means of measuring residence-time distribution of fluid in a fluidized bed. *Ingaku Kogaku*, 31, 239.
- Levy, G., & Teuner, S. (1990). Calcor process for CO production. *Erdöl und Kohle, Erdgas, Petrochemie vereinigt mit Brennstoff-Chemie*, 43, 171.
- Mieczko, J. A., & Jiang, X. (1992). Investigations of the mechanism of partial oxidation of methane to synthesis gas. *Preprint - American Chemical Society Division of Petrology Chemistry*, 37, 352.
- Nishiyama, M., Kado, H., Miyako, A., Nishiyama, S., & Tsuruya, S. (1988). Ethane reforming by carbon dioxide and steam over supported platinum, platinum and rhodium catalysts. *Studies in Surface Science Catalysis*, 36, 67.
- Orabekova, S. R., Mamedov, A. K., Aliev, V. S., & Krylov, O. V. (1992). Kinetics of conversion of C₁ - C₃ alkanes by carbon dioxide on organometallic compounds (russ.). *Kinetika Kataliz*, 33, 591.
- Mieczko, L., Malcus, S., & Wurzel, T. (1997). Catalytic reformer-combustor: a novel reactor concept for synthesis gas production. *Industrial and Engineering Chemistry Research*, 36, 4459.
- Mieczko, L., Ostrowski, T., & Wurzel, T. (1996b). A fluidised-bed membrane reactor for the catalytic partial oxidation of methane to synthesis gas. *Chemical Engineering Science*, 51, 3187.
- Mieczko, L., Pannek, U., Rothaemel, M., & Baerns, M. (1996a). Oxidative coupling of methane over a La₂O₃/CaO catalyst. Optimization of reaction conditions in a bubbling fluidized-bed reactor. *Canadian Journal of Chemical Engineering*, 74, 279.
- Mieczko, L., & Wurzel, T. (1997). Experimental Studies of Catalytic Partial Oxidation of Methane to Synthesis Gas in a Bubbling-Bed Reactor. *Chemical Engineering Journal*, 66, 193.
- Nguyen, U., Tangstad, E., & Dahl, I. M. (1994). Partial oxidation of ethane to synthesis gas in a fluidized bed reactor. *Studies in Surface Science Catalysis*, 81, 303.
- Nguyen, U., Wurzel, T., & Mieczko, L. (1997). Kinetic and reaction engineering studies of dry reforming of methane over a Ni/La/Al₂O₃ catalyst. *Industrial Engineering Chemistry Research*, 36, 5180.
- Peters, K., Rudolf, M., & Voetter, H. (1955). On the reaction pathway of methane reforming (germ.). *Brennstoff-Chemie*, 36, 257.
- Qin, D., Lapszewicz, J., & Jiang, X. (1994). Study of mixed steam and CO₂ reforming of CH₄ to syngas on MgO-supported metals. *Catalysis Today*, 21, 551.
- Richardson, J. T., & Paripatyadar, S. A. (1990). Carbon dioxide reforming of methane with supported rhodium. *Applied Catalysis*, 61, 293.
- Rostrup-Nielsen, J. R. (1994). Aspects of CO₂-reforming of methane. *Studies in Surface Science Catalysis*, 81, 25.
- Rostrup-Nielsen, J. R., & Bak Hansen, J. H. (1993). CO₂-Reforming of methane over transition metals. *Journal of Catalysis*, 144, 38.
- Santos, A., Menendez, M., Monzon, A., Santamaria, J., Miro, E. E., & Lombardo, E. A. (1996). Oxidation of methane to synthesis gas in a fluidized bed reactor using MgO-based catalysts. *Journal of Catalysis*, 158, 83.
- Seshan, K., ten Barge, H. W., Hally, W., van Keulen, A. N. J., & Ross, J. R. H. (1994). Carbon dioxide reforming of methane in the presence of nickel and platinum catalysts supported on ZrO₂. *Studies in Surface Science and Catalysis*, 81, 285.
- Solymosi, F., Kutsan, G., & Erdöhelyi, A. (1991). Catalytic reaction of methane with carbon dioxide over alumina-supported platinum metals. *Catalysis Letters*, 11, 149.
- Stansch, Z., Mleczko, L., & Baerns, M. (1997). Comprehensive kinetics of oxidative coupling of methane over the La₂O₃/CaO catalyst. *Industrial Engineering Chemistry Research*, 36, 2568.
- Swaan, H. M., Kroll, V. C. H., Martin, G. A., & Mirodatos, C. (1994). Deactivation of supported nickel catalysts during the reforming of methane by carbon dioxide. *Catalysis Today*, 21, 571.
- Teuner, S. (1985). Make CO from CO₂. *Hydrocarbon Processing*, 64, 106.
- Teuner, S. (1987). A new process to oxo-feed. *Hydrocarbon Processing*, 66, 52.
- Vernon, P. D. F., Ashcroft, T., Cheetham, A. K., & Green, M. L. H. (1991). Partial oxidation of methane to synthesis gas using carbon dioxide. *Nature*, 352, 225.
- Vernon, P. D. F., Green, M. L. H., Cheetham, A. K., & Ashcroft, T. (1992). Partial oxidation of methane to synthesis gas, and carbon dioxide as an oxidising agent for methane conversion. *Catalysis Today*, 13, 417.
- Wang, S., Lu, G. Q. (Max), & Millar, G. J. (1996). Carbon dioxide reforming of methane to produce synthesis gas over metal-supported catalysts: state of the art. *Energy and Fuels*, 10, 896.
- Wen, C. Y., & Yu, Y. H. (1966). A generalized method for predicting the minimum fluidization velocity. *A.I.Ch.E. Journal*, 12, 610.
- Werther, J. (1992). Scale-up modelling for fluidized bed reactors. *Chemical Engineering Science*, 47, 2457.
- Wurzel, T., & Mleczko, L. (1998). Engineering model of catalytic partial oxidation of methane to synthesis gas in a fluidized-bed reactor. *Chemical Engineering Journal*, 69, 127.
- Yu, Z., Choi, K., Rosynek, M. P., & Lunsford, J. H. (1993). From CH₄ reforming with CO₂ to pyrolysis over a platinum catalyst. *Reaction Kinetics Catalysis Letters*, 51, 143.
- Zhang, Z. L., & Verykios, X. E. (1994). Carbon dioxide reforming of methane to synthesis gas over supported Ni catalysts. *Catalysis Today*, 21, 589.

test1

```
it1
mass transfer coefficient
catalyst density calculation
pi*(dp/2)^2*h
m/vo
minimum fluidization velocity
=(1/180)*Emf^3*dp^2/(1-Emf)*(ps-pg)*g/vi
rate of reaction
4=0.25 ;
2=0.25 ;
=0.25 ;
2=0.15 ;
0.52 ;
10 ;
27 ;
2=(kco2-pch4*pcO2)/(1+k1*pch4+k2*pcO)*(1+k3*pcO2)
bubble velocity
=0.006 ;
11.8 ;
fn*umf
O2 profile
0.237 ;
4.7 ;
0 ;
mulsion phase
(1-fb)*gb*rco2/k
between 0 to 5
100:-0.1:0 ;
ot graph Ca vs z
t(z,Ca)
bel('Bed Height')
bel('CO2 Concentration')
le('Graph of CO2 concentration vs Bed Height')
d
```

test2

st2

mass transfer coefficient
for catalyst particle diameter 1 mm

catalyst density calculation

$$= \pi \cdot (dp/2)^2 \cdot h$$

$$= m/v_0$$

minimum fluidization velocity

$$= (1/180) \cdot Emf^3 \cdot dp^2 / (1 - Emf) \cdot (ps - pg) \cdot g/v_i$$

rate of reaction

$$r_4 = 0.25 ;$$

$$r_2 = 0.25 ;$$

$$r_3 = 0.25 ;$$

$$r_2 = 0.15 ;$$

$$= 0.52 ;$$

$$= 10 ;$$

$$= 27 ;$$

$$r_2 = (k_{CO_2} - p_{CH_4} \cdot p_{CO_2}) / (1 + k_1 \cdot p_{CH_4} + k_2 \cdot p_{CO} + k_3 \cdot p_{CO_2})$$

bubble velocity

$$f = 0.006 ;$$

$$= 11.8 ;$$

$$= 7.08$$

CO2 profile

$$= 0.237 ;$$

$$= 4.7 ;$$

$$= 0 ;$$

emulsion phase

$$= (1 - f_b) \cdot g_b \cdot r_{CO_2} / k$$

between 0 to 5

$$(r_{CO_2} \cdot g_b \cdot f_b + k \cdot dC) / (C_a \cdot U_b \cdot f_b)$$

$$= 100 : -0.1 : 0 ;$$

plot graph Ca vs z

plot(z, Ca)

xlabel('Bed Height')

ylabel('CO2 Concentration')

title('Graph of CO2 concentration vs Bed Height')

axis([0 1 0 100])

hold